NAVAL POSTGRADUATE SCHOOL

MONTEREY, CALIFORNIA

THESIS

INVESTIGATION OF THE ACOUSTIC SOURCE CHARACTERISTICS OF HIGH ENERGY LASER PULSES: MODELS AND EXPERIMENT

by

Jason R. McGhee

June 2008

Thesis Advisor: Daphne Kapolka

Approved for public release; distribution is unlimited

THIS PAGE INTENTIONALLY LEFT BLANK

REPORT DOCUMENTATION PAGE			Form Approved OMB No. 0704-0188
Public reporting burden for this collection of information is estimated to average 1 hour per response, including the time for reviewing instruction, searching existing data sources, gathering and maintaining the data needed, and completing and reviewing the collection of information. Send comments regarding this burden estimate or any other aspect of this collection of information, including suggestions for reducing this burden, to Washington headquarters Services, Directorate for Information Operations and Reports, 1215 Jefferson Davis Highway, Suite 1204, Arlington, VA 22202-4302, and to the Office of Management and Budget, Paperwork Reduction Project (0704-0188) Washington DC 20503.			
1. AGENCY USE ONLY *(Leave blank)*	**2. REPORT DATE** June 2008	**3. REPORT TYPE AND DATES COVERED** Master's Thesis	
4. TITLE AND SUBTITLE Investigation of the Acoustic Source Characteristics of High Energy Laser Pulses: Models and Experiment		**5. FUNDING NUMBERS**	
6. AUTHOR(S) Jason R. McGhee			
7. PERFORMING ORGANIZATION NAME(S) AND ADDRESS(ES) Naval Postgraduate School Monterey, CA 93943-5000		**8. PERFORMING ORGANIZATION REPORT NUMBER**	
9. SPONSORING /MONITORING AGENCY NAME(S) AND ADDRESS(ES) N/A		**10. SPONSORING/MONITORING AGENCY REPORT NUMBER**	
11. SUPPLEMENTARY NOTES The views expressed in this thesis are those of the author and do not reflect the official policy or position of the Department of Defense or the U.S. Government.			
12a. DISTRIBUTION / AVAILABILITY STATEMENT Approved for public release; distribution is unlimited.		**12b. DISTRIBUTION CODE**	

13. ABSTRACT (maximum 200 words)

This thesis was motivated by the possibility of using high energy laser pulses as an acoustic source for naval applications. Research conducted in the 1970's and 80's shows that sound production from laser pulses is most efficient when the energy density of the pulse exceeds the threshold required for plasma formation. The resulting acoustic wave falls into the highly non-linear shock regime. Later work by Vogel et al. sought a more complete understanding of the non-linear dynamics and energy distribution of this process in an attempt to limit collateral tissue damage during laser surgery. This work includes detailed experimental data including photographs and hydrophone measurements as well as numerical calculations of expected pressures, bubble dynamics, and pulse shapes.

The goal of this thesis was to investigate the characteristics of the laser generated acoustic pulse further through experimentation and modeling. Experiments were carried out with Ted Jones at the Naval Research Laboratory to investigate the directionality of the acoustic pulse produced by a 100fs 2mJ laser pulse focused just under the surface of water. The range dependence of the pressure amplitude was also examined. The amplitude of the pulse was found to vary with direction; however, this effect is considered likely to be a result of interference between the direct path and the surface reflection. A linear least-squares fit of the peak pressure amplitude with range revealed a $1/r^{1.2}$ relationship. This is consistent with the expected approximately 1/r relationship for pressure amplitudes under 100MPa. The modeling effort employed AUTODYN, a finite element program designed to handle the non-linear processes in explosions. The laser generated acoustic source was modeled using an explosive of the same volume as the laser spot reported by Vogel for his 10mJ 6ns pulse. The internal energy of the explosive was adjusted until the pressure amplitudes agreed with Vogel's measured values. The efficiency, pulse length, pulse shape, and variation of pressure amplitude with range achieved with AUTODYN are comparable to those reported by Vogel.

14. SUBJECT TERMS: Laser Acoustics, Shock Waves, Acoustic Sources, Nonlinear Acoustics, AUTODYN, Acoustic Modeling, Shock Acoustics	**15. NUMBER OF PAGES** 87
	16. PRICE CODE

17. SECURITY CLASSIFICATION OF REPORT	**18. SECURITY CLASSIFICATION OF THIS PAGE**	**19. SECURITY CLASSIFICATION OF ABSTRACT**	**20. LIMITATION OF ABSTRACT**
Unclassified	Unclassified	Unclassified	UU

NSN 7540-01-280-5500 Standard Form 298 (Rev. 2-89)
Prescribed by ANSI Std. 239-18

THIS PAGE INTENTIONALLY LEFT BLANK

Approved for public release; distribution is unlimited

INVESTIGATION OF THE ACOUSTIC SOURCE CHARACTERISTICS OF HIGH ENERGY LASER PULSES: MODELS AND EXPERIMENT

Jason R. McGhee
Lieutenant, United States Navy
B.S., University of Illinois, 1999

Submitted in partial fulfillment of the
requirements for the degree of

MASTER OF SCIENCE IN ENGINEERING ACOUSTICS

from the

NAVAL POSTGRADUATE SCHOOL
June 2008

Author: Jason R. McGhee

Approved by: Daphne Kapolka
Thesis Advisor

Kevin B. Smith
Chair, Engineering Acoustics Academic Committee

THIS PAGE INTENTIONALLY LEFT BLANK

ABSTRACT

This thesis was motivated by the possibility of using high energy laser pulses as an acoustic source for naval applications. Research conducted in the 1970's and 80's shows that sound production from laser pulses is most efficient when the energy density of the pulse exceeds the threshold required for plasma formation. The resulting acoustic wave falls into the highly non-linear shock regime. Later work by Vogel et al. sought a more complete understanding of the non-linear dynamics and energy distribution of this process in an attempt to limit collateral tissue damage during laser surgery. This work includes detailed experimental data including photographs and hydrophone measurements as well as numerical calculations of expected pressures, bubble dynamics, and pulse shapes.

The goal of this thesis was to investigate the characteristics of the laser generated acoustic pulse further through experimentation and modeling. Experiments were carried out with Ted Jones at the Naval Research Laboratory to investigate the directionality of the acoustic pulse produced by a 100fs 2mJ laser pulse focused just under the surface of water. The range dependence of the pressure amplitude was also examined. The amplitude of the pulse was found to vary with direction; however, this effect is considered likely to be a result of interference between the direct path and the surface reflection. A linear least-squares fit of the peak pressure amplitude with range revealed a $1/r^{1.2}$ relationship. This is consistent with the expected approximately 1/r relationship for pressure amplitudes under 100MPa. The modeling effort employed AUTODYN, a finite element program designed to handle the non-linear processes in explosions. The laser generated acoustic source was modeled using an explosive of the same volume as the laser spot reported by Vogel for his 10mJ 6ns pulse. The internal energy of the explosive was adjusted until the pressure amplitudes agreed with Vogel's measured values. The efficiency, pulse length, pulse shape, and variation of pressure amplitude with range achieved with AUTODYN are comparable to those reported by Vogel.

THIS PAGE INTENTIONALLY LEFT BLANK

TABLE OF CONTENTS

THIS PAGE INTENTIONALLY LEFT BLANK

LIST OF FIGURES

LIST OF TABLES

THIS PAGE INTENTIONALLY LEFT BLANK

I. INTRODUCTION

A. MOTIVATION

One of the biggest threats to a naval ship is a torpedo attack from an enemy submarine. Although an anti-torpedo torpedo (ATT) is in development, the only protection ships currently have against torpedoes is a combination of maneuvering the ship and the use of acoustic countermeasures. Even after the ATT is fielded, acoustic countermeasures will continue to be an important tool for surviving enemy torpedo attacks. These countermeasures can be deployed as expendable sources thrown over the side or as a towed source. The AN/SLQ-25 system, also known as Nixie, is an underwater acoustic source towed behind a ship and connected to an onboard signal generator by a coaxial cable. Nixie is capable of operating in a broadband mode to simulate the passive signature of a ship. It can also detect the torpedo's ping frequency, amplify it 2 to 3 times, and then retransmit it in an attempt to simulate the ship's echo and lure the torpedo away from the ship. The problem with Nixie is that it takes at least 15 minutes to deploy fully. If the ship is in known enemy submarine territory this is not a problem because Nixie is most likely already deployed, but Nixie provides no protection from a surprise attack. This suggests the advantage of having an acoustic countermeasure that is quick to deploy.

Much research has been done over the years on the use of high energy lasers (HELs) as a tool for anti-missile defense. Such lasers are being investigated as a possible replacement for the MK15 Phalanx Close-In Weapons System (CIWS), a shipboard missile defense system. In addition to causing ablation on the surface of an incoming missile, the energy in a laser pulse is also capable of producing sound through its interaction with water. Assuming that the laser was ready to fire, the speed with which sound could be produced by the laser far from the ship would be practically instantaneous. Therefore, it offers the possibility of being a valuable tool for anti-torpedo defense. Not only would it be faster than a towed system, but it might also eliminate the requirement for expendable countermeasures. To be a feasible countermeasure the laser-

generated source would need to be able to produce multiple frequencies in the kilohertz range and Sound Pressure Levels in the hundreds of decibels. The purpose of this thesis is to examine the sound produced by a high energy laser pulse to gain a better understanding of whether it might serve as a feasible acoustic source for torpedo countermeasures and/or other shipboard applications of underwater sound.

B. HISTORY

The idea that a light source could be used to produce sound was first proposed by Alexander Graham Bell. In his experiments, he showed that it was possible to generate sound waves in a medium that could absorb the light energy. This process became more interesting with the invention of the laser. In the 1980's, research into the use of air-mounted high energy pulsed lasers for missile defense led naturally to the investigation of this technology for a dual use in underwater acoustics. Some work also appears to have been motivated by Soviet research into laser-generated acoustics. In any case, several U.S. researchers including Bruce Maccabee from the Naval Surface Warfare Center Dahlgren, Ilene Busch-Visniac and Yves Berthelot from the Applied Research Laboratory in Austin, and Allan Pierce and H. Hsieh from the Georgia Institute of Technology all looked at the feasibility of using high energy pulsed lasers as acoustic sources. Interest in laser-generated sound was also motivated in the mid-1990s as lasers became a popular surgery technique. This led to experiments by A. Vogel, S. Busch, and U. Parlitz in which they investigated the shock waves produced by fairly low energy laser pulses in water. In the late 1990's, there is also evidence of interest in laser-generated acoustics for naval purposes among the Chinese. He and Feng from the Chinese Academy of Sciences in Shanghai and Duo-Min from Nanjing University described experimental work in which they produced sound in water using laser pulses. Duo-Min specifically mentions underwater acoustic communications as a possible application. Most recently, Ted Jones from the Naval Research Laboratory and his collaborators from a wide variety of government labs as well as private industry have developed some interesting new techniques to increase the achievable sound levels.

C. CONTRIBUTIONS OF THIS THESIS

Experiments were conducted for this thesis at the Naval Research Laboratory along with Ted Jones and his group at Code 6795. These experiments involved the use of a titanium-sapphire laser producing femtosecond pulses with an energy of about 2mJ and a wavelength of about 400nm. An analysis of these experiments includes an analysis of the apparent directionality of the laser-generated acoustic pulse and its range dependence.

The next part of this thesis involves an attempt to model the laser-generated acoustic pulse. The finite element program COMSOL Multiphysics was used at first; however, it is not designed to handle non-linear processes. For this reason, the decision was made to switch to AUTODYN. AUTODYN is also a finite element program, but it is specifically designed to handle the non-linear effects involved with high energy explosions. When the energy of a laser pulse is deposited quickly enough into a small volume of water, it evaporates and ionizes the water. This causes a rapid expansion in the volume of the bubble, which produces a shock wave. AUTODYN was used in an attempt to model this shock wave.

D. ORGANIZATION

Chapter II of this thesis includes a more detailed review of the existing background work on laser-generated acoustic sources. The focus of this chapter is on the physics of this process and the acoustic pressures, which have been achieved. Chapter III on Theoretical Acoustic Pulse Estimates provides a qualitative summary of the characteristics of both the laser pulse and the acoustic medium, which affect the amplitude, shape, length, and directionality of the acoustic pulse. It also presents some issues with previous attempts to quantify where the initial electro-optic energy ends up. Chapter IV follows with a description of the experimental set-up for the work done at the Naval Research Laboratory and an analysis of the results. Chapter V explains the modeling effort. It goes through the various approaches tried in AUTODYN to model the shock wave generated by the laser pulse. This discussion also includes some insights

into the limitations of AUTODYN for this particular application. Chapter VI discusses the conclusions to be drawn from this work, and recommendations for future work are provided in Chapter VII.

II. BACKGROUND

In this chapter, the background work mentioned in the introduction will be explored in greater detail. An overview of the relevant work will be provided as well as details concerning the theory developed and the experimental values obtained.

A. OVERVIEW OF PREVIOUS WORK

During the 1980's, there was considerable interest in high energy lasers as a possible technology for missile defense. In particular, the feasibility of mounting high energy lasers on board aircraft was examined. This interest raised the question as to whether the lasers could be used for other applications as well. Building on the theoretical and experimental work of both US and Soviet research in the late 1970's, at least three U.S. groups looked at this issue. Yves Berthelot and Ilene Busch-Visniac from the Applied Research Laboratories, The University of Texas at Austin [1985] investigated the acoustic wave generated by a laser source moving over the water at speeds ranging from subsonic and supersonic. Allan Pierce and H. A. Hsieh of the Georgia Institute of Technology [1986] proposed an approach designed to tailor the directionality of the acoustic signal by the careful placement and timing of laser beams on the ocean surface. Bruce Maccabee [1987] from the Naval Surface Warfare Center Carderock Division provided the theory for linear pressure waves resulting from simple, single laser pulses as well as experimental data on the pressures obtained. The interest in airborne laser systems diminished in the 1990's most likely due to a drop in the funding for this form of strategic missile defense; however, interest in laser generated sound resurfaced in the mid to late 1990's with the increasing popularity in laser surgery. German scientists A. Vogel, S. Busch, and U. Parlitz [1996] published an article with a theoretical treatment of the shock waves produced by the laser pulses in water as well as their experimental observations. This work was motivated by a desire to understand the potential tissue damage attendant to laser surgery – particularly in the eye. Chinese researcher, He Duo-Min of the Nanjing University of Science and Technology showed renewed interest in the use of laser generated sound for submarine communications in a

1998 paper delivered at a Strategic Research Seminar in Singapore. Two other Chinese researchers, H. He and S. Feng at the Chinese Academy of Sciences in Shanghai [1999], also showed an interest in laser generated acoustics; however, they were using the phenomenon as a means of investigating the optical response time of the water through its ability to focus an intense laser beam by changes in its refractive index. Also in the late 1990's, Ted Jones, Jacob Grun, Ray Burris, and Charles Manka [1999] published a technical report at the Naval Research Laboratory (NRL) which was to be the starting point for a program designed to explore and improve the acoustic signal which could be generated using high energy laser pulses. By 2006, this effort led to a novel idea for increasing the intensity of the laser pulse in water, i.e., the use of a reverse chirp in conjunction with dispersion to shorten the pulse in the direction of propagation.

Of these early works, several will be explored in more detail. The basic theory of the laser-water interaction will be presented for both linear and shock waves. In addition, the basic ideas for improving the performance of a laser acoustic source will be explained and a comparison of the experimental data obtained by various groups will be provided.

B. MECHANISMS FOR LASER-GENERATED SOUND

Maccabee [1987] proposed that the mechanisms for laser generated sound be divided into four types. It is important to distinguish these different types, because the theory as well as the efficiency of the process varies substantially depending on the nature of the laser-water interaction. The first type occurs when the laser energy heats the water but is not high enough to cause evaporation. The electro-optic to acoustic efficiency for this type of interaction is approximately 0.01%. The second type occurs when the absorbed energy is high enough to cause evaporation. This rapid evaporation causes the volume to expand very fast and produces a larger pressure than in the first type. The efficiency for Type 2 is higher than the Type 1 at 0.1-1%. The third type is where the laser energy is so high that it ionizes the water. The formation of a plasma allows the water to absorb more of the laser energy, thus causing the volume to expand faster and to a larger final radius. This type has the highest efficiency at 10-30%. The final type of laser generated acoustics is produced by focusing the laser onto an

underwater object. For this case, the frequency of the laser should be one that has the lowest absorption coefficient in water so that most of the laser energy will be absorbed by the underwater object instead of the water. From here, the process is similar to type one. The absorption of laser energy will cause the object's temperature to increase, which will cause it to expand rapidly producing a pressure wave. Since the efficiency of the Type 4 process depends on the particulars of the object, Maccabee does not speculate on the range of efficiencies which might be expected from it.

Maccabee provides some interesting experimental data of the pressure waves produced by laser pulses. This data was taken 4.9 cm below the laser pulse, and the results are shown in the graph below. The cross-sectional area of the spot remained constant at $0.2cm^2$. The pulse length was changed between the third and fourth graphs, and measurements were not made of the spot volume. Thus, the exact energy densities are unknown. However, it is clear from the plots that at low laser pulse energies, the acoustic pulse assumes a bipolar shape while at higher energies it starts to show a shock front. The acoustic pressure goes below an absolute pressure of zero. This is possible only when the timeframe of the process is too quick for evaporation to occur, i.e., the water is in tension. At yet higher pulse energies, the negative pressure swing disappears and a shock wave with exponential tail appears.

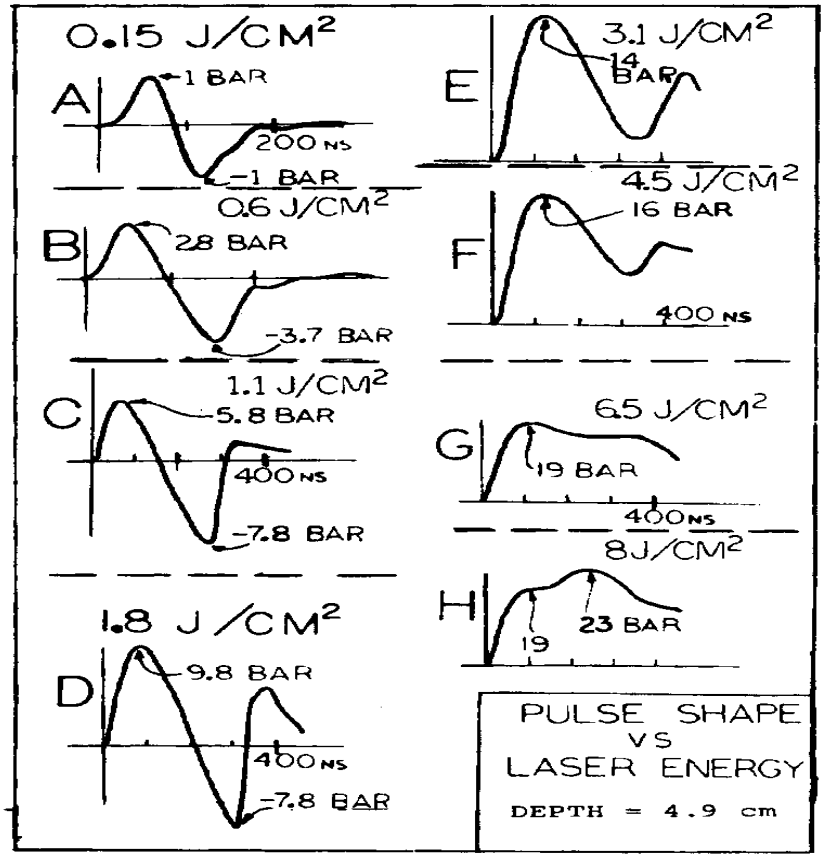

Figure 1 Experimental results of the pressure wave received 4.9 cm below laser spot for varying amounts of laser pulse energies. (From: Maccabee, 1987)

Of the types of laser sound production mentioned by Maccabee, Type 1 (heating) and Type 3 (ionizing) are of the most interest. Type 1 is of interest because it can be described by linear theory. Type 3 is of interest, because the efficiency of the electro-optic to acoustic conversion is substantially higher than Type 1 or 2. Type 4 (focusing energy onto an object) is potentially interesting, but the details would depend on the nature of the object used. Therefore, only Type 1 and 3 interactions will be examined in more detail.

C. TYPE 1 SOUND PRODUCTION – LINEAR THEORY

When a laser pulse deposits energy in water such that the energy density is below the threshold required for evaporation, the water expands proportionally to the

temperature increase and the volume coefficient of expansion. The theory for determining the pressure and directionality of the resulting pressure wave is identical for any mechanism which heats water. Sulak et al. [1979], for example, derive an expression for the acoustic wave resulting from the interaction of a proton beam with water. Interestingly, they point out that at temperatures below 6°C, the coefficient of expansion for water is negative thus resulting in a pressure pulse, which has a rarefaction preceding the compressional wave. Two other observations from this paper are worth noting for this thesis. One is the formula for the pressure amplitude expected from the instantaneous, uniform heating of a long, thin rod-shaped volume of water. The expression (attributed to Dolgoshein and Askarian) is:

$$p(r,\theta) = \frac{K}{C_p}\frac{E}{r}\frac{c^2}{8d^2}\frac{\sin\left(\frac{\pi L}{2d}\sin\theta\right)}{\frac{\pi L}{2d}\sin\theta}, \qquad \text{Eqn 1}$$

where K is the volume coefficient of expansivity, C_p is the heat capacity of water, E is the total energy deposited, r is the distance from the rod (in the far field), c is the velocity of sound, d is the diameter of the rod, L is the length of the beam, and θ is the angle measured relative to the normal to the rod. Although this formula is specifically for the uniform heating of a rod, a maximum will occur at $\theta = 0^o$ for any linear energy deposition where the timescale of the energy deposition is fast compared to the acoustic timescale. This is due to the fact that the contribution to the pressure from all points along the line will be in phase along the acoustic axis. Therefore, if a laser pulse were to penetrate deeply into the water creating a long line of heating with an exponential decay, one would still expect to get a pressure maximum normal to the laser beam. Sulak [1979] also provides an equation he attributes to Bowen for the pressure amplitude as a function of time. It is:

$$p(\vec{r},t) = \frac{K}{4\pi C_p}\frac{\partial}{\partial t}\int dV \frac{w(\vec{r},t-r/c)}{r}, \qquad \text{Eqn 2}$$

where $w(\vec{r},t)$ is the heat power per unit volume deposited at $\vec{r}$ at time t, dV is an infinitesimal unit of the heated volume, and r is the magnitude of the distance to the point where the pressure is measured. From this formula, it can be seen that for a finite laser pulse in the time domain, the pressure depends on how quickly the heat power is changing.

The other observation worth noting is that the pulse expected from this heating is a bipolar pulse with a period equal to the time required for the pressure wave to travel from the back of the heated volume to the front along the line of observation plus the energy deposition time.

Maccabee [1987] also derives an expression for the pressure expected from heating water. His treatment is different from the one we see in Sulak, because he looks specifically at a situation where there is an exponential decay in intensity along the laser beam. The intensity of the laser beam in water at depth z is given by the equation

$$I(z) = I_0 e^{-\alpha z} \qquad \text{Eqn 3}$$

where α is the attenuation coefficient of water and I_0 is the laser intensity at the surface.

Differentiating both sides of this equation with respect to depth yields

$$\frac{dI}{dz} = -\alpha I_o e^{-\alpha z} = -\alpha I(z). \qquad \text{Eqn 4}$$

Since the change in intensity of the beam is due to the power absorbed by the water, the power absorbed can be expressed as:

$$\frac{dE}{dt} = -\frac{dI}{dz} S\, dz = -\frac{dI}{dz} dV \cong \alpha I(z) \Delta V ,$$

where S is the cross-sectional area of the beam and ΔV is the small volume in which the power of the beam is deposited.

This absorbed power causes both the temperature and volume of the water to increase according to

$$\frac{1}{\Delta V}\frac{d^2V}{dt^2} = \beta \frac{d^2T}{dt^2}, \qquad \text{Eqn 5}$$

where β is the coefficient of volume expansion and $\frac{d^2V}{dt^2}$ is the acceleration of the volume increase. Furthermore, the change in temperature with respect to time is related to the heat capacity of the water, the volume, and the power absorbed as:

$$\frac{d^2T}{dt^2} = \frac{d}{dt}\left(\frac{dE/dt}{\rho \Delta V C_p}\right) \qquad \text{Eqn 6}$$

where ρ is the density of water and C_p is the specific heat per unit mass. (It is assumed here that the heat capacity and density of the water do not change during the heating process.) Substituting the expression for power above yields:

$$\frac{d^2T}{dt^2} = \frac{d}{dt}\left(\frac{\alpha I(z)\Delta V}{\rho\, \Delta V\, C_p}\right) = \frac{d}{dt}\left(\frac{\alpha I(z)}{\rho\, C_p}\right). \qquad \text{Eqn 7}$$

Rearranging the above equations yields the acceleration of the volume expansion

$$\frac{d^2V}{dt^2} = \alpha\beta \frac{d}{dt}\left(\frac{\alpha I(z)}{\rho\, C_p}\right)\Delta V. \qquad \text{Eqn 8}$$

This is not the expression that Maccabee gives in his paper. He omits the time derivative and gives the acceleration of volume expansion as:

$$\frac{d^2V}{dt^2} = \alpha\beta \frac{\alpha I(z)}{\rho\, C_p}\Delta V. \qquad \text{Eqn 9}$$

This is clearly an error, since it is not dimensionally correct.

Maccabee goes on to give the infinitesimal contribution to the pressure from the acceleration of the volume expansion in the far-field as:

$$dp(t) = \frac{\alpha\beta e^{-\alpha z}}{4\pi r C_p} I_0(t - r/c)dV, \qquad \text{Eqn 10}$$

where $\left(t - r/c\right)$ is the standard retarded time, i.e., the time at which the pressure contribution from dV arrives at range r. Integrating this expression over the heated volume would yield:

$$p(\vec{r},t) = \frac{\beta}{4\pi r C_p}\int_L \alpha I_0(t - r/c)e^{-\alpha z} S dz, \qquad \text{Eqn 11}$$

where L is the length over which the beam deposits its energy. This expression would be identical to the one provided in Sulak's paper if the derivative with respect to time had not been dropped from the formula and if the heat power deposited per unit volume had an exponential decay with distance, i.e., $w\left(t - r/c\right) = \alpha I\left(t - r/c\right) = \alpha e^{-\alpha z} I_o\left(t - r/c\right)$. Therefore, the correct equation for Maccabee's case should be given as:

$$p(\vec{r},t) = \frac{\alpha\beta}{4\pi r C_p}\frac{\partial}{\partial t}\int_L I_0(t - r/c)e^{-\alpha z}Sdz\,. \qquad \text{Eqn 12}$$

This is an important correction, because it predicts that the pressure produced depends on how quickly the intensity changes with time. Assuming that the heat capacity, linear expansion coefficient, and attenuation remain constant, an increase in pressure can be attained in Type 1 sound generation either by increasing the energy of the laser pulse while keeping the pulse length constant, or by maintaining the pulse energy while decreasing the pulse length.

D. TYPE 3 SOUND PRODUCTION – SHOCK WAVES

Since the most efficient conversion of laser power to acoustic power occurs when the energy density is high enough to produce a plasma, this type of sound production is more interesting in terms of its potential as an acoustic source. Unfortunately, under these conditions, the resulting acoustic wave falls into the shock regime. Therefore, the theory describing it is more complicated. Moreover, the factors affecting the fraction of laser power which is converted to an acoustic pulse are only partly understood. The best attempt to describe the complex shock wave produced by a high energy laser pulse is that of Vogel et al. [1996, 1999]. The motivation of their work is to understand the effects of intraocular laser surgery and, in particular, to find a regime in which the collateral damage caused by the expanding bubble and shock wave is minimized. The pulse energies are fairly small; however, since the energy densities were high enough to produce Type 3 behavior, their treatment is relevant to this thesis. Of course, the goal of laser acoustics is exactly the opposite of intraocular surgery. To create the maximum possible acoustic signal, laser pulse parameters, which maximize the transformation of

laser energy into mechanical energy are desirable. The insights gained from Vogel's work are a valuable starting point for laser acoustics, but further work is needed to ensure that they are equally valid for higher energy pulses.

To summarize Vogel's insights into the interaction between laser pulses and water, a timeline of the interaction will be presented along with an analysis of the factors which affect the efficiency of the energy conversion from laser to mechanical energy. Although they investigated the process for several different wavelengths ranging from 532 nm to 1064 nm, they found virtually no difference in the behavior as a function of incident wavelength. This is not too surprising since the laser pulses only penetrated the fluid for a short distance before reaching the focal point. Thus, frequency dependent absorption was not an issue. This would certainly not be the case for an application in which the laser pulse penetrated significant distances into the fluid before focusing.

When a laser pulse enters water, the absorption coefficient is fairly low until a threshold energy density is met, which causes the water to ionize into a plasma. Once the plasma is formed, the density of free electrons keeps the light absorption extremely high as long as the plasma frequency is not exceeded. If this were to happen, the plasma would become perfectly reflecting. This explains the substantially higher efficiency which Maccabee noted for the Type 3 process. The intensity first becomes high enough to form a plasma at the focal point. Later, as the pulse intensity rises, the plasma grows toward the laser beam where the beam cross-sectional area is larger. Since the cross-sectional area of the beam increases faster for larger focusing angles, the threshold intensity required to ionize the water can only be achieved close to the focal point. For smaller focusing angles, the threshold intensity is met at greater distances. This results in a larger initial plasma spot size and lower energy density than the larger focusing angle achieves. This concept is illustrated in Figure 2. Here, the laser beam enters from the right. The apex of the cone is the focal point where the threshold is first exceeded before the laser pulse reaches its maximum. As the laser pulse builds in amplitude, the threshold is reached at larger and larger cross-sectional areas until the maximum amplitude of the pulse occurs. For the larger focusing angle on the right, this cross-sectional area is

achieved closer to the apex. Since the volume of a cone is given by $\frac{1}{3}\pi r^2 h$, where r is the radius of the base, the plasma volume for the larger focusing angle is smaller. The fact that the plasma is growing in volume towards the beam tends to keep electron densities below the plasma frequency thus contributing to the ability of the water to absorb the incident light energy.

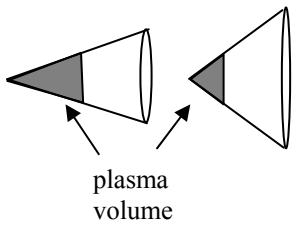

Figure 2 Diagram of plasma volume for small (left) and large (right) focusing angles.

The size of the initial plasma spot is not only dependent on the focusing angle. It also depends on the laser pulse length. For pulses containing the same total energy and shape, the peak intensity of a shorter pulse must be greater than the peak intensity of a longer pulse. This results in a larger plasma volume since, again, the intensity reaches the threshold value further away from the focal point. There is a limit to the extent to which the pulse can be lengthened to obtain a smaller volume, because the intensity has to exceed the threshold in order to get sufficient absorption. Vogel et al. [1999] provide a graph of the percent of laser energy transmitted through the fluid as a function of the total pulse energy for a 30ps pulse length and various focusing angles. This graph is shown below. At lower pulse energies transmission is very high since the threshold has not been reached. As the energy exceeds the threshold required for ionization, the transmission becomes smaller as larger amounts of the laser pulse energy are absorbed in the plasma. It is worthwhile to note that the improvement in the percent of energy absorbed is minimal after the threshold energy has been exceeded by a factor of about 50. For laser pulse lengths on the order of nanoseconds and below, the absorption timeframe is fast in comparison to the rate of heat conduction and shock wave propagation. Therefore, immediately following the laser pulse, the laser energy absorbed by the water is still

confined to a volume roughly equal to the initial spot size. Since the laser pulse timeframe is small compared to the consequent thermodynamic and mechanical processes, the subsequent evolution is relatively insensitive to the initial laser pulse length.

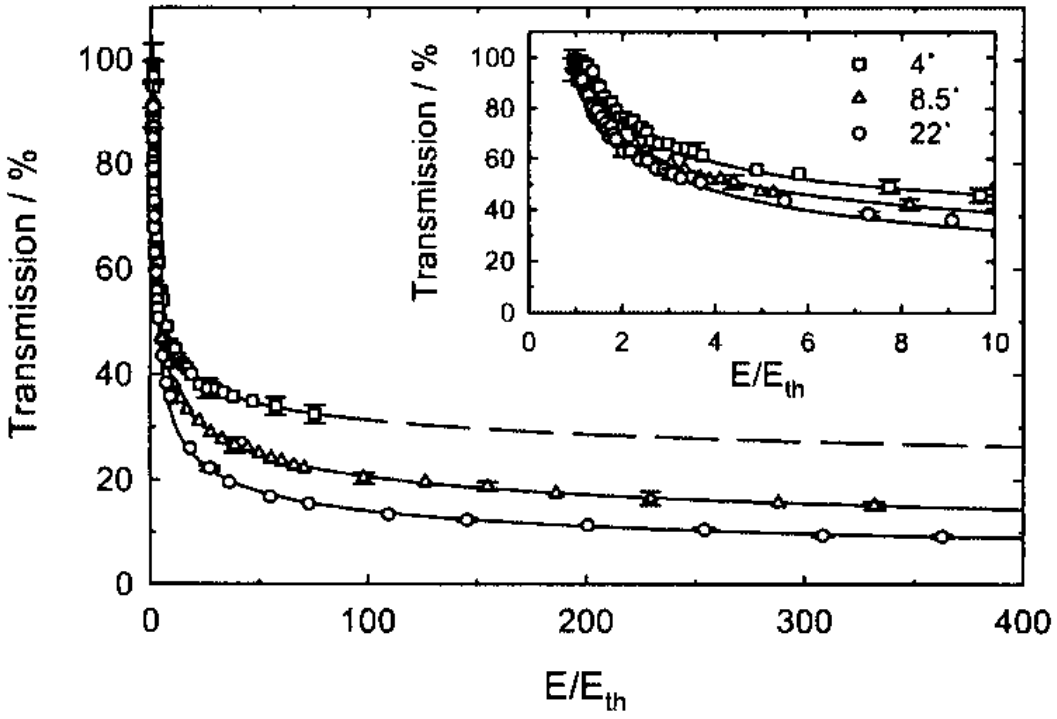

Figure 3 Percent transmission versus normalized energy for a 30ps pulse at various focusing angles. (From: Vogel et al. [1999])

Vogel calculates the energy required to heat the water in the plasma volume to the boiling point and then vaporize it as:

$$E_V = \rho_o V_p \left[c\left(T_2 - T_1\right) + r \right], \qquad \text{Eqn 13}$$

where V_p is the plasma volume, ρ_o is the density of water, c is the heat capacity of water, T_2 is the boiling point, T_1 is the initial temperature of the water, and r is the specific heat of vaporization of water. No mention is made of the energy required to create the plasma or raise it to its final temperature at the end of the laser pulse. Presumably, this is due to the assumption that this energy is completely converted to

mechanical energy in the form of the bubble expansion and shock wave. They do investigate the energy, which is lost to plasma radiation based on the Stefan-Boltzmann Law. However, despite the high plasma temperature, the energy lost to radiation was found to be negligible in all cases.

The energy density within the plasma volume causes it to heat up, vaporize, and expand. The free electrons collide and transfer their energy to the heavier ions. High speed photographs of the process reveal that the shock front detaches from the plasma immediately after its formation. They also show a roughly spherical shock front and cavitation bubble. The photograph below shows a long cavitation bubble and the shock front surrounding it produced by a 1mJ 30ps pulse in the upper right. In comparison, the 1mJ 6ns pulse on the bottom left shows a shorter, more symmetrical cavitation bubble and shock front. Assuming that the size of the cavitation bubble and shock front are proportional to the initial spot size, this photograph thus demonstrates the inverse relationship between plasma spot size and pulse length.

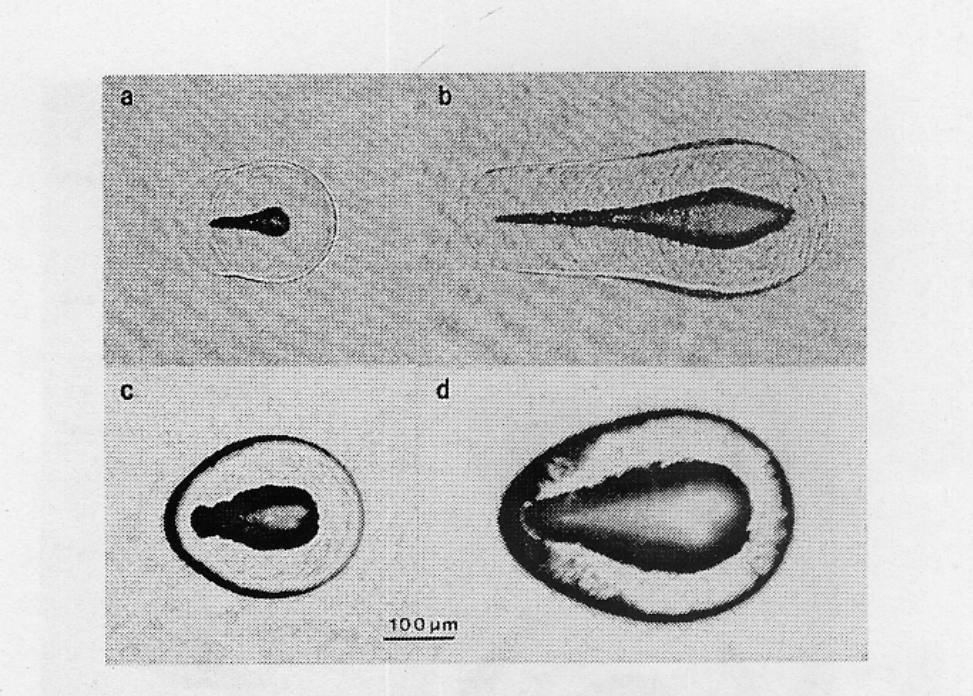

Figure 4 Photograph of cavitation bubble and shock wave 44ns after pulse. (From: Vogel et al. [1996])

The percentage of the laser pulse energy, which is converted into the mechanical energy of the cavitation bubble and shock wave, depends strongly on the initial energy density. On the other hand, Vogel found that the ratio of the energy between the shock wave and the bubble were remarkably constant at about 2:1 over a wide range of pulse energies and lengths (from a $50\,\mu J$ pulse with a 30ps duration to 10mJ and 6ns.) Since the bubble energy is fairly easy to measure from its maximum expansion radius, they recommend its use in determining the fraction of the laser pulse energy which is transformed into mechanical energy. The expression used for the bubble energy is given as [Vogel et al. 1999, p. 273]:

$$E_B = \frac{4}{3}\pi R_{\max}^3 \left(p_o - p_v \right), \qquad \text{Eqn 14}$$

where $R_{\max}$ is the maximum radius obtained, ρ_o is the hydrostatic pressure of the water the bubble expands against, and ρ_v is the vapor pressure of the water. They use a hydrostatic pressure of 0.1MPa (1 atm) corresponding to a bubble near the surface of the water and a vapor pressure of 2330Pa at 20^0C. Vogel does not derive this formula, but it can be derived from:

$$W = \int_{V_i}^{V_f} p dV \,. \qquad \text{Eqn 15}$$

This is the standard formula for the work, W, done by a gas expanding against a constant external pressure. Direct application of the formula would yield:

$$W = \int_{V_i}^{V_f} p dV = p_o \left(\frac{4}{3}\pi R_{\max}^3 - V_i \right). \qquad \text{Eqn 16}$$

To obtain the formula they give, $p_o V_i$ must be equated with $p_v V_f$. This is equivalent to starting with an ideal gas with initial volume, V_i, at hydrostatic pressure and allowing it to expand at a constant temperature until the external pressure is equal to the vapor pressure of water. The expansion of the plasma to create a cavitation bubble is hardly an equilibrium process, nor would it be isothermal. Moreover, the equation of state for the highly condensed, hot plasma probably does not obey the ideal gas law. However, the correction for the initial volume is likely to be small for cases where the conversion of

energy to mechanical is efficient. At the very least, one would expect the maximum bubble volume to be proportional to the energy which drives the bubble expansion. Vogel et al. [1999] provide a graph of the percent of the laser pulse energy, which is converted to bubble energy. This graph, shown below, shows the dramatic effect of laser pulse length. As the energy is raised further and further above threshold, there is little change in the conversion efficiency at any of the pulse lengths.

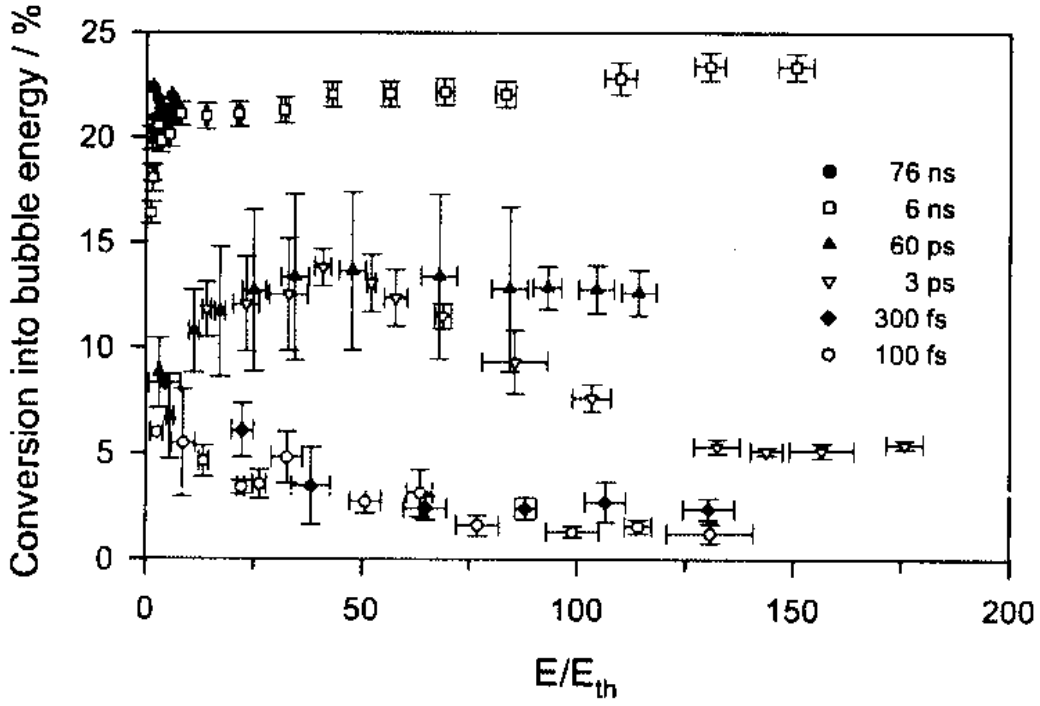

Figure 5 Percent of laser pulse energy converted into cavitation bubble as a function of pulse length and normalized pulse energy. (From: Vogel et al. [1999])

Due to the difficulties inherent in measuring the amplitude of the shock wave close to the laser pulse, Vogel and his collaborators rely on an interesting interplay of theory and experiment to determine the portion of energy, which goes into the shock wave. This was used to verify the 2:1 proportioning of energy between the shock wave and the cavitation bubble. A graph of the shock wave as a function of time is shown below. It shows the classic initial shock and exponential tail of the shock wave. The width of the shock wave appears to be correlated with the pulse energy.

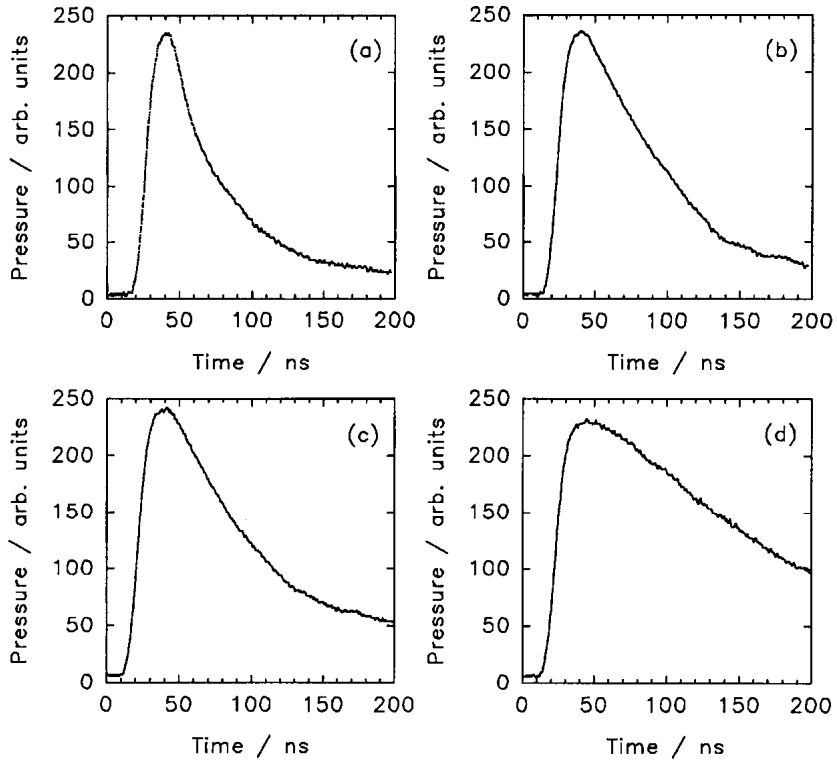

Figure 6 The shock wave measured 10mm from the plasma volume for (a) 30ps, 50 μ J; (b) 30ps, 1mJ; (c) 6ns, 1mJ; (d) 6ns, 10mJ. (From: Vogel et al. [1996])

The expression used by Vogel [1999] for the energy in the shock wave is:

$$E_S = \frac{4\pi r^2}{\rho_0 c_0} \int p^2 dt \,, \qquad \text{Eqn 17}$$

where ρ_o is the nominal density of water and c_o is the nominal sound speed. The pressure can be measured directly by a small hydrophone with a quick response time at distances starting at about 10mm from the laser pulse. At shorter ranges, direct measurement of the pressure is very difficult. Therefore, they used a couple of different techniques to try to estimate the pressure closer in. The first technique uses the maximum radius of the cavitation bubble, the laser pulse length, and the plasma volume to predict the evolution of the pressure wave in the surrounding liquid. Based on the

Gilmore model of cavitation bubble dynamics, calculations were performed to predict the pressure at a range equal to six times the initial plasma radius. Using the pressure from this calculation in combination with the equation for the energy in a shock wave above yields the shock wave energy, $E_S^{Gilmore}$. They also computed the shock wave energy using a different technique for comparison purposes. The other technique uses the energy left 10mm from the center (where the curvature of the wavefront is large enough to be measured with a small hydrophone) and the energy dissipated as the shock wave travels from its initial position at the edge of the plasma volume out to a range of 0.3mm. The energy remaining at 10mm is referred to as $E_{S/10mm}$, and the energy dissipated up to 0.3mm is referred to as E_{Diss}. The equation used for the dissipation of energy is based on the Rankine-Hugoniot equations. The increase in internal energy of the medium through which a shock wave passes is given by:

$$\Delta\varepsilon(r) \cong \frac{1}{2}\left(\frac{1}{\rho_o} - \frac{1}{\rho_s(r)}\right) p_s(r), \qquad \text{Eqn 18}$$

where ρ_s is the density of the shock wave and p_s is the pressure of the shock wave. Using conservation of mass at the shock front and an equation of state they attribute to Rice and Walsh, the pressure of the shock wave can be derived from the velocity of the shock front as:

$$p_s = c_1 \rho_o u_s \left(10^{(u_s - c_o)/c_2} - 1\right) + p_o \qquad \text{Eqn 19}$$

where c_o is the normal sound of sound in water, c_1 = 5190m/s, c_2 = 25,306m/s, ρ_o = 998kg/m^3, and p_o is hydrostatic pressure. They were able to measure the velocity of the shock front photographically; however, as the velocity approaches the nominal speed of sound, the uncertainty of the pressure calculation becomes large. Therefore, they only used this method to calculate the dissipation out to 0.3mm. From the increase in internal energy, they calculate the energy dissipated as:

$$E_{Diss} = \int_{r_0}^{r_1} 4\pi r^2 \rho_s(r) \Delta\varepsilon(r)\, dr\,, \qquad \text{Eqn 20}$$

where r_o is the radius at the onset of the shock wave formation and r_1 is the final radius included. The density at the shock front is calculated from the expression for the conservation of mass:

$$u_s \rho_o = (u_s - u_p)\rho_s \qquad \text{Eqn 21}$$

and the expression for the conservation of momentum:

$$p_s - p_o = u_s u_p \rho_o\,, \qquad \text{Eqn 22}$$

where u_p is the particle velocity behind the shock front. They claim that this method underestimates the energy in the shock wave since it fails to include dissipation from 0.3mm to 10mm. However, they still find that it predicts a higher shock wave energy for all cases than the Gilmore method. They attribute this discrepancy to the possibility that more energy is lost in the early phases of the shock wave – before the Gilmore method can be accurately applied – than in the 0.3 - 10mm region that is omitted in the dissipation method. More will be said in the theory chapter about potential problems with these attempts to pin down the shock wave energy.

Other conclusions from Vogel's work of interest to the present study are as follows:

- As much as 96% of the incident laser energy is absorbed by the plasma volume for a 6ns 10mJ pulse [Vogel et al. 1999, p. 275].
- As much as 69% of the absorbed energy goes into the shock wave for a 6ns 10mJ pulse [Vogel et al. 1999, p. 275].
- 85-89% of the shock wave energy is dissipated in the first 0.2 – 0.3mm of shock wave propagation [Vogel et al. 1999, p. 275].
- Pressure decays as r^{-2} until the pressure falls below 100MPa [Vogel et al. 1996, p. 148].
- After the pressure falls below 100MPa, the pressure falls as approximately r^{-1} [Vogel et al. 1996, p. 148].

To the extent that these estimates are correct, the maximum expected efficiency of the electro-optic to acoustic conversion is approximately:

$$96\% \times 69\% \times 11 - 15\% = 7 - 10\% .$$

This represents the conversion of the laser pulse into useful acoustic energy after the strongly dissipative initial stages of the shock wave have passed.

Since the interest in this study is on the pressure amplitudes obtainable at longer ranges, it is also useful to examine more closely the measured shock wave parameters at 10mm. Again, using the later (1999) paper and the more efficient 6ns pulse, the results can be summarized in the following table.

Table 1 Experimental data measured at 10mm for 1mJ and 10mJ laser pulses with length of 6ns. (From: Vogel et al. [1999]) Efficiency computed from Vogel data.

Laser Energy	1mJ	10mJ
Pressure (MPa)	0.99	2.62
Duration (ns)	77	148
Energy (μJ)	46.2	622
Efficiency of conversion (laser/acoustic wave at 10mm)	5%	6%

Note that the pressures at 10mm are below 100MPa. Therefore, the pressure is expected to fall as $1/r$ as the range increases.

E. IDEAS FOR SHAPING THE ACOUSTIC PULSE

In addition to Maccabee's early suggestion to focus the laser energy on an underwater object, there are two other innovative ideas increasing the efficiency and/or directionality of the laser acoustic source, which should be mentioned. The first of these techniques, specifically developed with airborne laser sources in mind, seeks to maximize

the acoustic signal through the placement of successive pulses. The second technique, recognizing that efficiency is proportional to the energy density of the plasma, seeks to reduce the plasma volume through non-linear self-focusing and the use of a reverse chirp signal.

The idea of moving the source to take advantage of the summation of successive pulses was studied both theoretically and experimentally by Bertholet and Busch-Visniac [1985]. They recognized that by moving the laser spot location at speeds exceeding Mach 1, the wavefronts from successive pulses would reinforce each other and create a higher amplitude signal than could be achieved by a single pulse. To test this, they used a rotating mirror to move the beam across the surface of the water. They also modulated the signal by using a Pockels cell. The experimental results showed a maximum increase of 20dB in the pressure amplitude over what could be achieved with a stationary source. They also developed an ingenious makeshift modulation technique when the Pockels cell failed. By laying a pattern of wooden sticks across the surface of the water, they were able to modulate the laser amplitude as it scanned the water surface at the appropriate Mach number to achieve the desired wavefront summation.

More recently, Jones et al. [2006] reported two techniques, which could be used to increase the electro-optic to acoustic conversion efficiency. Noting that the efficiency is largely dependent on the energy density of the plasma volume, Jones's group proposed using two different techniques, the reverse chirp and nonlinear self-focusing to maximize the energy density of the resultant plasma.

These techniques work in different dimensions to decrease the size of the initial laser spot. Nonlinear self-focusing (NSF) relies on the non-linearity of the refractive index at high intensity to provide a focusing effect in the water medium. This results in a constriction in the transverse dimension. At the same time, a constriction along the longitudinal dimension is achieved by taking advantage of the dispersive properties of water. By starting out with a negatively chirped laser pulse, the group velocity dispersion of water causes a longitudinal compression as shown in the figure below. Unfortunately,

the beam has to travel a relatively large distances to achieve the required focusing, i.e., about 8m for the experiments conducted by Jones. This results in some attenuation in the pulse energy based on the wavelength of the laser pulse employed.

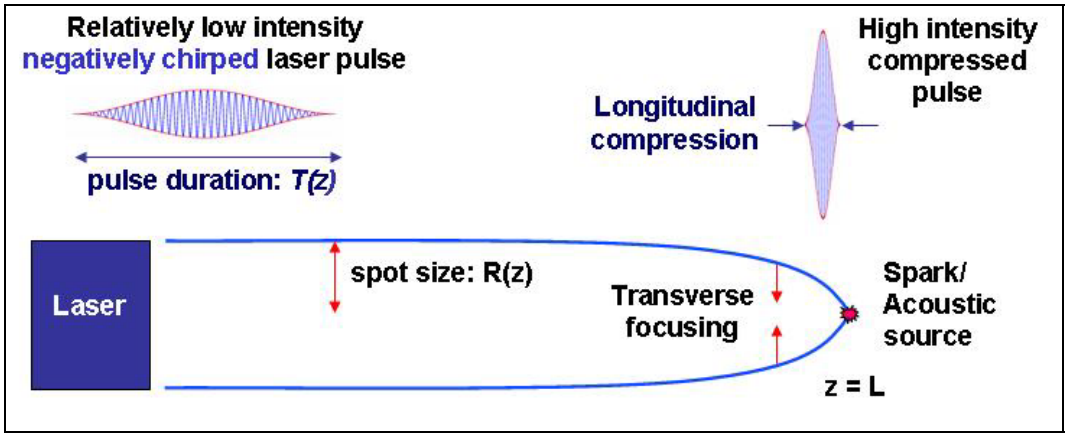

Figure 7 Transverse and longitudinal focusing from a negatively chirped laser pulse in water (From: Jones et al. 2006)

F. EXPERIMENTAL RESULTS

Several factors that affect the efficiency of the electro-optic to acoustic conversion were discussed in the previous sections. At a general level, efficiency is affected by pulse length, focusing angle, total pulse energy, and wavelength (for pulses that penetrate into the water.) To get a quick overview of the pressure amplitudes, which were achieved by various research groups, the peak amplitudes from their "best shots" are presented in the graph below as a function of pulse energy. In order to make the comparisons meaningful, the pressure amplitude is extrapolated to a range of 1m. This is justified in that all measurements were taken for pressure amplitudes below 100MPa, the transition point between $1/r^2$ and $1/r$ spreading. Following the graph, a table is provided to detail the parameters, which resulted in the plotted measurement.

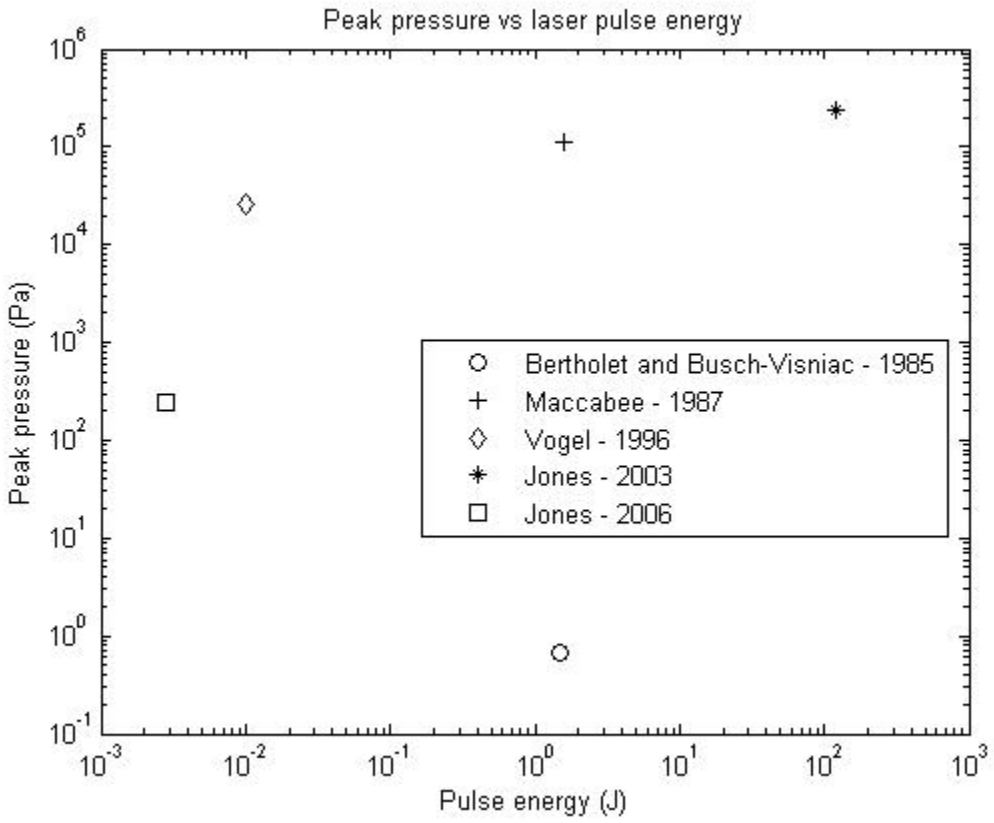

Figure 8 Peak pressures achieved by various research groups. Values are extrapolated to a range of 1m using $1/r$ spreading.

Table 2 Parameters used to achieve peak pressures shown in Figure 8

Group	**Pulse energy**	**Pulse length**	**Spot Size**	**Focusing**	**Comments**
Bertholet and Busch-Visniac [1985]	1.5J	1.2ms	$0.8cm^2$	not focused	1.38Pa at 0.5m 1.06 μ m wavelength $\alpha = 13.7m^{-1}$ no shock wave
Maccabee [1987]	1.6J	200ns	$0.2cm^2$	focused on surface	2.3MPa at 4.9cm directly below 10.6 μ m wavelength "Type 2" - evaporative
Vogel et al. [1996]	10mJ	6ns	$45 \mu m^2$	focused - 22^0 convergence angle	2.62MPa at 10mm 1.06 μ m wavelength
Jones et al. [2003]	120J	5ns	$0.2 - 0.5cm^2$	focal length of 2m	18MPa at 13mm 527nm wavelength $\alpha = 0.02m^{-1}$ focused on plastic foil
Jones et al. [2006]	2.8mJ	50fs	unknown	unknown	49kPa at 5mm 400nm wavelength $\alpha = 0.1m^{-1}$

Since the peak intensity of the acoustic signal should be roughly proportional to the energy in the laser pulse, it is also interesting to form a relative figure of merit (FOM) as the peak pressure squared divided by the pulse energy. This FOM fails to take into consideration the duration either of the acoustic pulse or any asymmetries in the radiation pattern. However, these factors were not provided by all groups. Therefore, the FOM defined in this way cannot be used as a precise measure of the conversion efficiency. Table 3 shows the FOM calculated from the data above.

Table 3 Ratio of peak pressure squared to laser pulse energy achieved by various research groups.

Group	FOM $\left(p_{pk}^2 / E_{laser} \right)$
Bertholet and Busch-Visniac [1985]	**0.32** Pa^2/J
Vogel et al. [1996]	$6.9\times10^6\ Pa^2/J$
Jones et al. [2006]	$2.1\times10^7\ Pa^2/J$
Jones et al. [2003]	$4.8\times10^8\ Pa^2/J$
Maccabee [1987]	$7.6\times10^9\ Pa^2/J$

From the FOM data shown above, clearly the result from Bertholet and Busch-Visniac shows the smallest conversion efficiency from electro-optic to acoustic energy. This is consistent with a Type 1 heating process resulting from the long pulse length and consequently low peak laser intensity. Maccabee's 1.6J shot shows the highest conversion efficiency even though he considers it to be the result of a Type 2 evaporative process on the surface of the water. This is a surprising result and raises the question of whether the process was purely Type 2, or whether there was plasma formation as well. The 2003 shot of Jones et al. shows that a much higher energy pulse (120J) can also achieve very high conversion efficiencies when the plasma spot size is minimized through the use of a foil target. This group's 2006 shot shows just an order of magnitude lower conversion efficiency with a much shorter pulse length and no foil. Finally, Vogel et al. achieved a conversion efficiency about an order of magnitude lower than Jones [2006]. This is somewhat surprising since their beam was focused, and they used a

longer pulse length. According to Vogel, both of these factors should have contributed to the smaller spot size and higher initial energy density associated with a high conversion rate.

III. THEORETICAL ACOUSTIC PULSE ESTIMATES

The physics of the interaction between a high energy laser pulse and water is not understood well enough to calculate the exact details of the acoustic wave produced based solely on the laser pulse parameters, placement of the pulse, and physical properties of the water. It is not even clear that the problem can be well bounded due to the number of factors involved. However, it is possible to develop some intuition into the factors, which affect the characteristics of the acoustic pulse. Therefore, the first section of this chapter lists all the factors either which have been shown or which are considered likely to play a part in determining the characteristics of the resultant acoustic pulse. These factors are then discussed in an attempt to clarify the roles they play in determining the acoustic pulse. The last section of this chapter looks at several of Vogel's calculations in more detail and speculates qualitatively about the effect of the assumptions made on the conclusions drawn from that work.

A. FACTORS AFFECTING THE ACOUSTIC PULSE PRODUCED BY A HIGH ENERGY LASER PULSE

In general, the parameters which affect the acoustic signal produced by a high energy laser pulse can be divided into two basic categories, i.e., the laser pulse characteristics and the characteristics of the acoustic medium. In some cases the effect of these characteristics are inextricably linked.

1. Laser Pulse Characteristics

The laser pulse characteristics, which determine the resultant acoustic signal, can be summarized as:

- Total energy per pulse
- Pulse length in time domain
- Pulse shape in time domain
- Pulse cross-section
- Focus angle

- Wavelength
- Angle of incidence into medium
- Pulse repetition rate

While the total energy of the laser pulse sets an upper limit to the energy which ends up in the resultant acoustic signal, other factors can cause the percent energy conversion to vary from almost 0% to a high of about 10%. For example, operating at a wavelength, which suffers little absorption in water, causes the energy transmission through the water to be very high. Thus, little of the incoming electro-optic energy is converted into an acoustic pulse. On the other hand, if the energy density is high enough to form a plasma, more of the electro-optic energy is absorbed. The resulting heating and vaporization of the water transfers energy to the acoustic wave. This plasma formation is the key to obtaining high efficiencies since even wavelengths which absorb well in water will not deposit sufficient energy in a small enough volume to attain good conversion efficiencies. In general, the greater the energy density in the water immediately following the laser pulse, the greater the efficiency of the electro-optic to acoustic conversion. For a given total pulse energy, the peak intensity of the laser pulse is inversely proportional to its duration. Therefore, smaller pulse lengths in the time domain tend to result in higher efficiencies. On the other hand, if the energy density is too high, electron densities may be high enough to exceed the plasma frequency. In this case, all remaining electro-optic energy would be reflected. Thus the upper limit to the energy density is determined by the point where the plasma frequency is reached. All other factors being equal, it might be possible to harness more of the energy of a pulse by shaping it in such a way that a plasma is formed very early so that absorption is high throughout the following pulse evolution. The changing speed of light in the water as a function of the heating, vaporization, ionization, and pressure is another issue, which affects the shape of the electro-optic pulse as it travels though the water. Jones et al. [2006] have suggested how the natural dispersion of the medium can be harnessed to increase the energy density of a reverse chirp pulse. In general, however, refraction of the laser light away from regions of lower density/higher temperatures and scattering off bubbles has not been considered. It is likely that these effects would be more important

for multiple pulses directed in rapid succession at the same area. Since multiple pulses will be required for achieving low frequency acoustic signals, refraction and scattering issues may be important.

The cross-section of the laser beam also plays an important role in the energy density attained. The cross-section of the beam in the water depends on the original cross-sectional characteristics of the beam as well as the distance to the water, atmospheric conditions affecting the beam propagation, difference in refractive index of water and air, beam focusing, and, again, as pointed out by Jones et al. [2006] the non-linear self-focusing effect. Since the efficiency of the conversion is dependent on whether the energy density is high enough to create a plasma, efficiency is favored by having a cross-sectional area small enough to attain the threshold energy density required for ionization. External focusing with large focusing angles led in Vogel's work to higher efficiencies since the cross-sectional area required to reach the threshold energy density occurred closer to the focal point. This resulted in a higher overall energy density of the pulse.

The amount of the original pulse energy, which enters the water, depends on the transmission coefficient of the air/water interface. This coefficient depends on the angle of incidence and the indices of refraction for water and air. Of course, it also depends on how smooth the surface is. For ocean applications, the surface of the ocean might be locally smooth in the vicinity of the laser beam, but the angle of incidence would be fairly random. On the other hand, since the speed of light is slower in water than it is in air, there is no critical angle at which the transmission coefficient goes to zero.

2. Characteristics of Acoustic Medium

The characteristics of the acoustic medium, in this case water, which affect the ability of the medium to transform the electro-optic energy from the laser pulse into acoustic energy can be summarized as:

- Speed of sound (which is a function of temperature, pressure, and salinity)
- Density
- Viscosity

- Heat capacity
- Heat conduction
- Heat of Vaporization
- Ionization energy
- Shape and location at which electro-optic energy is deposited

As the laser energy is absorbed by the water, it heats up. If the timeframe of the laser pulse is fast compared to the time it takes for heat to conduct away or for vaporization to occur, the spot where the energy is deposited can be envisioned as superheated, ionized water. The temperature of the water is determined by the heat capacity of the water at constant volume and by the energy lost to ionization and heat conduction over the timeframe of the laser pulse. This superheated water is going to expand. Vogel's experimental evidence shows almost no loss of energy in the form of radiation. This is probably due to the density of the water in the laser spot. Collisions between electrons and ions most likely lead to a quick recombination and the consequent transfer of the energy to heat. This fast conversion of the energy lost to ionization back to heat energy would also explain why Vogel did not include any mention of ionization energy in his energy balance.

The expanding spot creates a shock wave, which detaches almost immediately from the bubble of vaporized water. The bubble will continue expanding until its internal pressure is balanced by the external pressure. It will then oscillate with damping and gradually get reabsorbed in the water as the temperature decreases.

The details of the shock wave propagation depend on the speed of sound in water at the various local temperatures and densities as well as the small viscosity of the water. Energy is lost to the shock wave due to heat conduction. The placement of the pulse relative to the surface of the water plays an important role in the received acoustic signal since it reflects the acoustic pulse with a 180^0 phase shift.

B. ENERGY BALANCE

Since it is impossible to predict the precise acoustic characteristics expected based solely on the characteristics of the input laser pulse and the water, an understanding of the energy balance of the process is particularly valuable. In this regard, several of the equations used by Vogel et al. [1996, 1999] bear further examination.

To start with, Vogel et al. [1999] give the following figures for the energy balance of their 6ns 10mJ pulse:

- Energy reflected off laser spot – 0.8%
- Energy scattered off laser spot – 0.5%
- Energy transmitted though laser spot – 2.6%
- Energy absorbed by water – 96.1%
- Mechanical energy needed to form bubble – 29.4%
- Shock wave energy – 49.3 – 68.5% (depending on how measured)
- Energy of Vaporization – 6.5%
- Energy radiated – 6 x 10^{-4}%
- Energy unaccounted for – 1.3%

The energy reflected off, scattered by, and transmitted through the laser spot are measured by calibrating a receiver by assuming that 100% of the light incident on the sample at low energies is transmitted. Thus, these measurements do not include energy lost at any of the optical interfaces other than the laser spot itself.

The energy of vaporization is calculated using the equation:

$$E_V = \rho_o V_p \left[c\left(T_2 - T_1\right) + r \right], \qquad \text{Eqn 23}$$

where $\rho_o V_p$ is the volume of the laser spot, c is the heat capacity, and r is the latent Heat of Vaporization. As noted previously, this equation does not account for the energy required to attain temperatures above the boiling point of water at atmospheric pressure, 100^0C. It assumes that only the water in the volume of the initial laser spot is vaporized. They use the Heat of Vaporization and the heat capacity for isobaric processes. The assumption that the heating and vaporization are isobaric processes and the use of values

measured for equilibrium processes at specific temperatures are not accurate for this non-equilibrium process. Furthermore, since the temperature of the bubble is likely to be considerably higher than 100^0C, this approach is expected to underestimate the energy required to vaporize and heat the water.

The energy required to form the cavitation bubble is calculated using the equation:

$$E_B = \frac{4}{3}\pi R_{\max}^3 \left(p_o - p_v \right), \qquad \text{Eqn 24}$$

where, again, $R_{\max}$ is the maximum radius obtained, ρ_o is the hydrostatic pressure of the water the bubble expands against, and ρ_v is the vapor pressure of the water. Again, the issue with the use of this formula is that using $dW = pdV$ to calculate the work done by an expanding gas assumes an equilibrium process.

The energy of the shock wave is also a difficult calculation to do under the conditions of a non-equilibrium process. Vogel does this calculation in two different ways – both of which admittedly underestimate the energy in the shock wave. One uses the measurement of the pressure at a distance of 10mm to calculate the energy left at this point. That quantity is added to the energy dissipated up to a range of 0.3mm. This method is considered to underestimate the initial energy in the shock wave because dissipation from 0.3mm to 10mm is not included. The other method used to estimate the energy in the shock wave is to use the equation:

$$E_S = \frac{4\pi r^2}{\rho_0 c_0} \int p^2 dt \,. \qquad \text{Eqn 25}$$

Since the pressure cannot be measured directly close to the laser spot, the pressure was estimated using the Gilmore model and experimentally determined values for the maximum bubble radius, laser spot size, and pulse duration. Aside from any questions on the ability of the Gilmore model to predict the shock wave pressure, it should be pointed out that the equation used above for the energy in a shock wave is derived from linear acoustics. It comes from the fact that the instantaneous intensity, $I(t)$, of an acoustic wave is given by:

$$I(t) = p(t)u(t), \qquad \text{Eqn 26}$$

where $u(t)$ is the particle velocity. For a linear, spherical wave, the magnitude of the pressure and particle velocity is given by KFCS by:

$$p(t) = \frac{A}{r}\cos(\omega t - kr) \qquad \text{Eqn 27}$$

and

$$u(t) = \frac{1}{\rho_o c}\frac{A}{r}\frac{1}{\cos\theta}\cos(\omega t - kr - \theta), \qquad \text{Eqn 28}$$

where $\frac{A}{r}$ is the amplitude of the pressure at range r, ω is the angular frequency, k is the wavenumber, and θ is the phase difference between the pressure and particle velocity. For a spherical wave, this phase difference depends on range and is given by:

$$\tan^{-1}\frac{1}{kr}. \qquad \text{Eqn 29}$$

This is significant, because at very small values of kr, the pressure and particle velocity are close to 90^0 out of phase. Thus, high particle velocities yield little in the way of acoustic pressure for small acoustic sources. Integrating the instantaneous intensity over one period yields the expression:

$$I = \frac{P^2}{2\rho_o c}, \qquad \text{Eqn 30}$$

where P is the pressure amplitude at range r. For a finite wave containing different frequencies, each frequency component would behave the same, thus yielding the expression given by Vogel. However, the relationship between pressure and particle velocity is incorrect in the highly non-linear regime of shock waves. The relationship between pressure and particle velocity given by Vogel as:

$$p_s = c_1\rho_o u_s\left(10^{(u_s - c_o)/c_2} - 1\right) + p_o \qquad \text{Eqn 31}$$

should be used instead to estimate the energy in the shock wave.

THIS PAGE INTENTIONALLY LEFT BLANK

IV. EXPERIMENTS

Experiments were conducted with Ted Jones at the Naval Research Laboratory, Code 6795 during the week of July 23-27, 2007, using a Ti:sapphire laser. The goal of these experiments was to get a preliminary understanding of the equipment and procedures involved in laser-generated acoustics as well as to do some rough measurements of the acoustic signal generated by a fairly low energy pulse. The experiments were successful in measuring the pressure and its range dependence starting at a range of a few centimeters from the source. Experiments were also conducted to get a feel for the directionality of the acoustic source; however, these were inconclusive due to the possible role of surface interference in determining the received pressure amplitudes.

The pulses used in these experiments had an approximate pulse length of 100fs, a 400nm wavelength, and an approximate energy of 2mJ. They were directed into an open air water tank that had a volume of $1m^3$. The tank was approximately half full and the pulse was directed at the surface of the water using mirrors and lenses. A diagram of the optical set-up is shown in Figure 9, and a photograph of the equipment is shown in Figure 10.

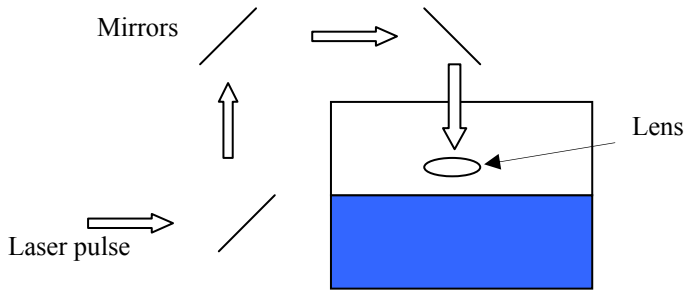

Figure 9 Diagram of Experimental Setup.

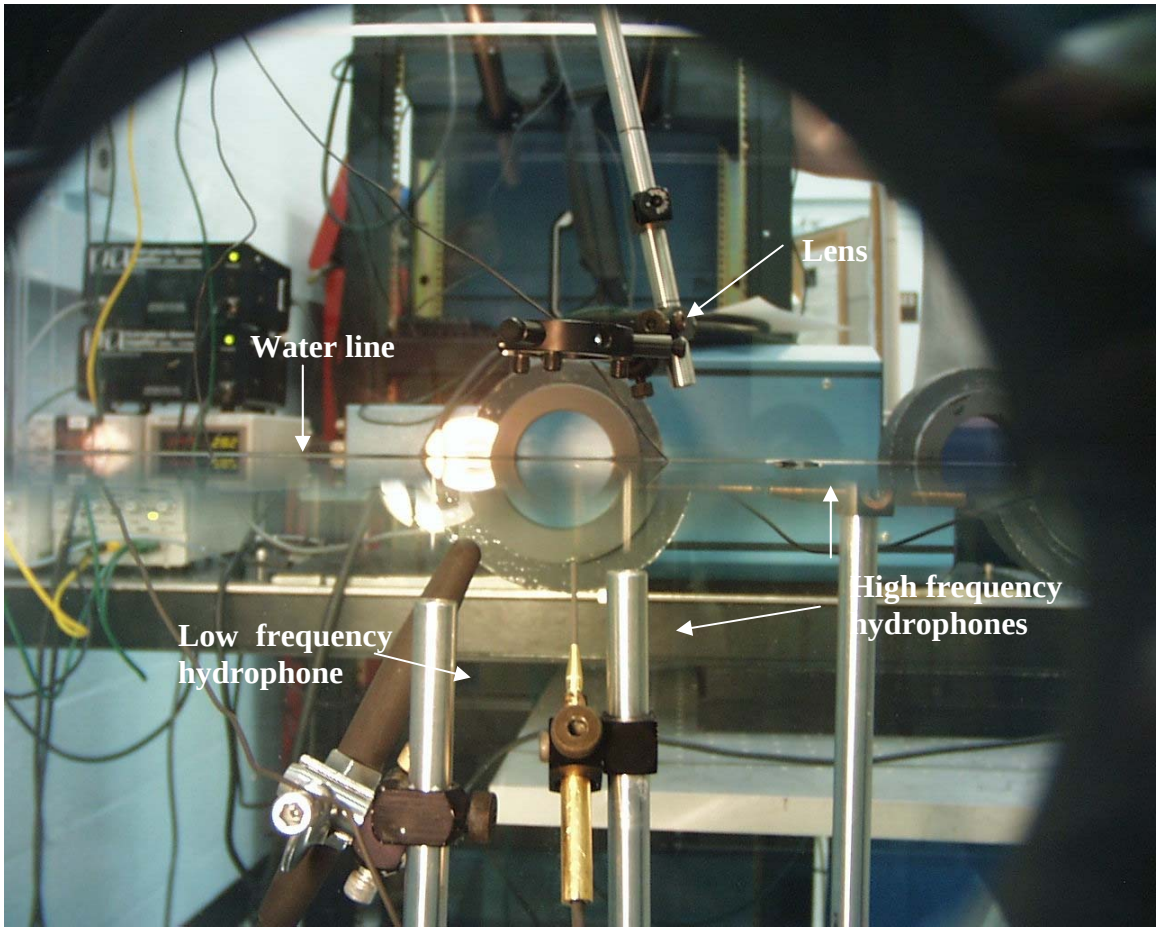

Figure 10 Picture of experimental setup.

A negatively chirped laser pulse was not used in any of these experiments so no longitudinal compression of the laser beam was expected once the laser hit the water. Also, because the tank was not deep enough for nonlinear self focusing (NSF) to occur, a lens was used to focus the laser. The lens was moved up and down in an attempt to focus the laser just below the surface of the water, but without the use of a high speed camera it was very difficult to tell with the naked eye if the laser spot was on or below the surface of the water. Instead, the lens was moved until a maximum response was observed on the oscilloscope. A telescope was used to make the cross section of the beam larger to prevent energy loss from the beam and damage to the mirrors and lenses due to

filamentation. Filamentation is caused by self focusing of the laser beam which results in intensities high enough to produce a plasma. The plasma formation in air removes energy from the laser beam before it reaches the water.

Acoustic data was obtained using a low frequency hydrophone and two high frequency hydrophones. The low frequency hydrophone was a TC-4034 manufactured by Reson. The hydrophone was connected to the oscilloscope through a VP1000 preamplifier also manufactured by Reson. The high frequency hydrophones were 1mm needle hydrophones manufactured by Precision Acoustics LTD. They were connected to the oscilloscope through HA60 preamplifiers also manufactured by Precision Acoustics LTD. Using the voltage from the oscilloscope, V, the pressure, P, was determined using the sensitivity, M, of the hydrophones from the hydrophones' calibration curves provided in the Appendix along with the preamplifier gain, G, in dB.

$$P = \frac{V}{M(10^{\frac{G}{20}})} \qquad \text{Eqn 32}$$

A. DIRECTIONALITY STUDY

The first experiment conducted was an attempt to determine the directionality of the acoustic pulse from a laser-generated acoustic source using the high frequency hydrophone. The received pulse is shown in Figure 11. It can be seen in this figure that the period of the pulse is about $1.1\,\mu s$, which leads to a pulse frequency of about 0.91 MHz.

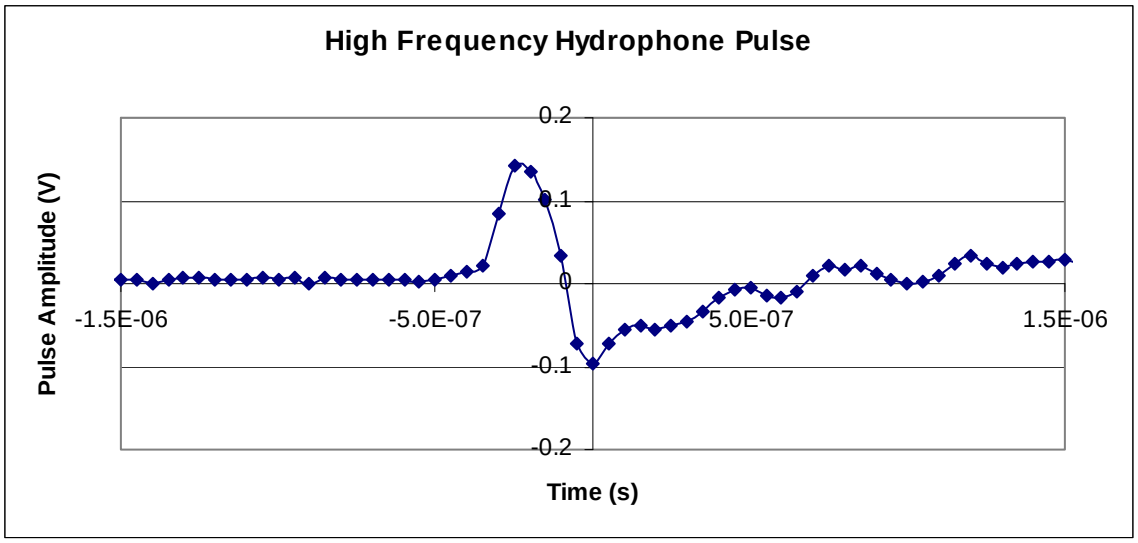

Figure 11 Pulse shape from high frequency hydrophone achieved during the 30^0 directionality trial.

Since there was no high speed camera available to photograph the interaction of the laser pulse with the water, it was impossible to measure the precise distance between the laser spot and the hydrophone. Therefore, the position of the hydrophone was adjusted until the elapsed time between the initiation of the laser pulse and the arrival of the acoustic pulse at the hydrophone was approximately the same at each angle. The angle itself had to be estimated with a protractor by assuming the location of the laser spot was on the surface of the water along the beam direction. Care was taken to point the hydrophone as close to directly at the laser spot as possible while using the naked eye. However, based on the relatively flat, 1MHz line on the directionality plot for the high frequency hydrophone in the Appendix, the pointing direction of the hydrophone should not make a noticeable difference. A basic diagram is shown in Figure 12.

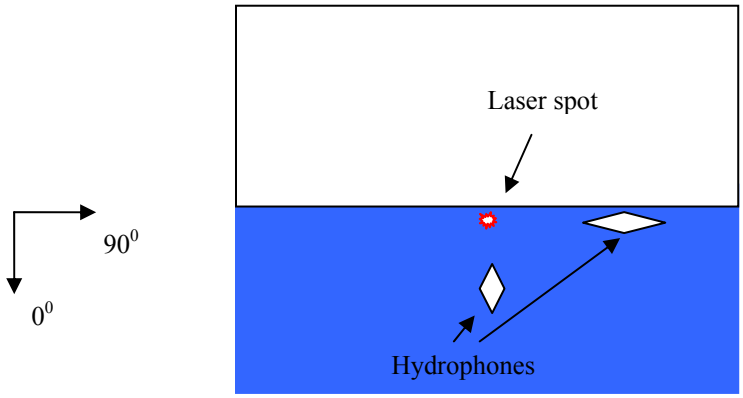

Figure 12 Diagram of basic setup for directionality experiment.

The results are shown in Figure 13 with 0^o being directly below the laser spot. Each angle shows the data from three laser pulses except for 45^0 where the data from two of the pulses was corrupted. The hydrophone was not moved between pulses at each angle. The peak pressures attained from these trials were higher at 0^0 and 30^0 and then fell off at sharply at 45^0 and above. This observation might be consistent with a directional pulse if the beam entered the water at an angle such that the mainlobe of the beampattern occurred around 30^0, and if the pulse energy were deposited along a line whose length was larger than its diameter. However, the pulse was focused onto a small spot, and the direction of entry was nominally normal to the surface. Therefore, it is more likely that the observed drop in peak pressure is due to interference between the direct acoustic pulse and its reflection off the surface.

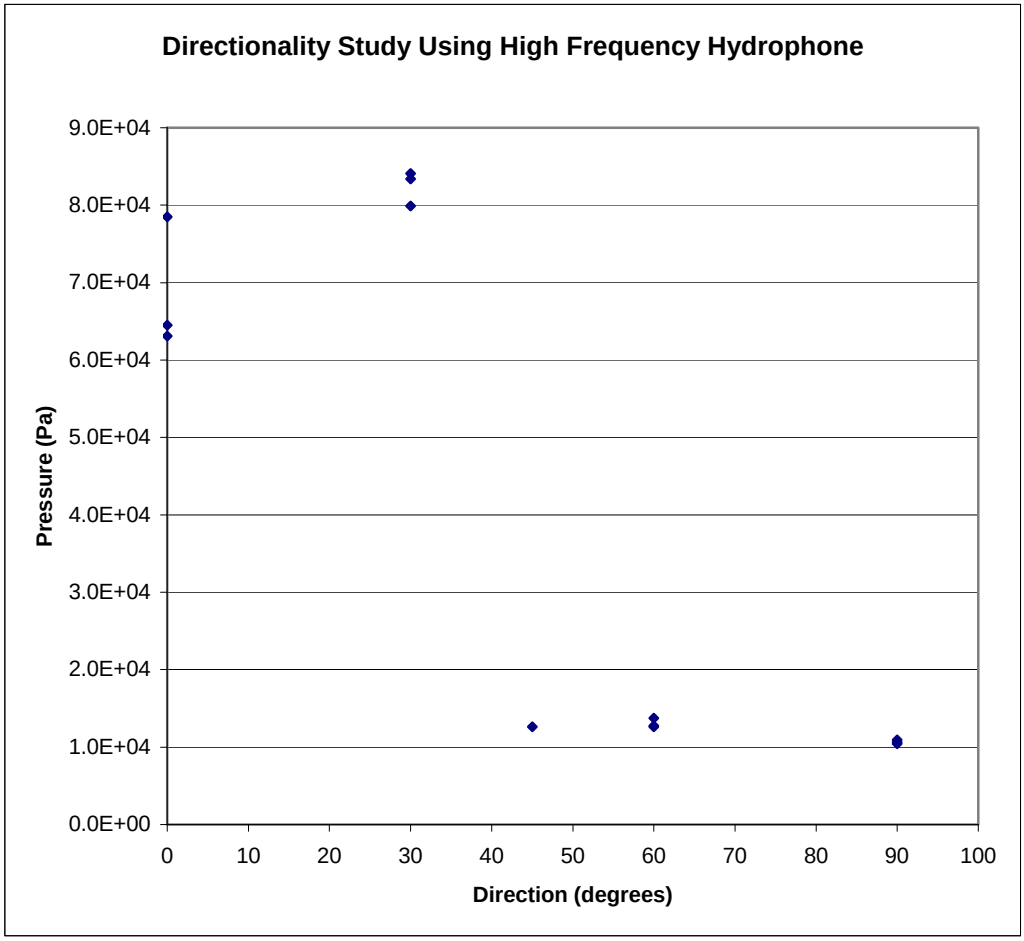

Figure 13 Directionality study of laser-generated acoustic source using a high frequency hydrophone.

The effect of surface interference can be explained by an analysis of the diagram shown below.

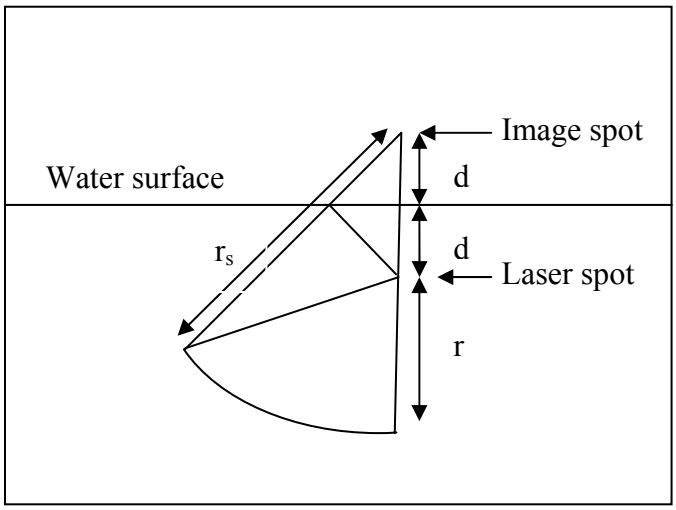

Figure 14 Surface interference geometry for calculating the path length difference between direct and surface reflected path.

The laser pulse is deposited at a depth of d beneath the surface and a hydrophone is located at a range r and an angle θ from it. The surface reflection travels a longer distance, r_s, to the hydrophone. Using the Pythagorean Theorem, the length of the reflected path can be expressed in terms of the source depth, hydrophone separation, and angle as:

$$r_s^2 = r^2 \sin^2\theta + \left(2d + r\cos\theta\right)^2. \qquad \text{Eqn 33}$$

Multiplying this out and simplifying leads to:

$$r_s^2 = r^2 + 4rd\cos\theta + 4d^2. \qquad \text{Eqn 34}$$

When d is much less than r then this can be further simplified to:

$$r_s^2 \cong r^2 + 4rd\cos\theta = r^2\left(1 + \frac{4d\cos\theta}{r}\right). \qquad \text{Eqn 35}$$

Since the cosine has a maximum value of one and d is assumed to be small, the length of the reflected path can be approximated by:

$$r_s \cong r\left(1 + \frac{2d\cos\theta}{r}\right). \qquad \text{Eqn 36}$$

Thus, the path length difference between the direct and reflected path can be approximated as:

$$r_s - r \cong 2d\cos\theta\,. \qquad \text{Eqn 37}$$

The maximum path length difference, $2d$,occurs when $\theta = 0^0$ which is when the hydrophone is directly below the laser spot. The minimum path length difference occurs when $\theta = 90^0$, or when the hydrophone is perpendicular to the laser direction. Since the direct and reflected path lengths are 180^0 out of phase due to the phase shift resulting from the air-water impedance difference, the two paths interfere destructively if they arrive simultaneously. With the measured temporal pulse length of $1.1\,\mu s$, the physical length of the pulse (assuming a propagation speed of 1480m/s) is about 1.6mm. Path length differences less than about a millimeter would allow the negative part of the reflected pulse to arrive during the compressional part of the direct path pulse. For example, if the laser spot were focused at a depth of 1mm, the path length between the direct and reflected path would be about 1mm at an angle of 60^0. At smaller angles, the path length difference would be larger, and the pulses would start to separate. Therefore, the fact that the pressure dropped off significantly at larger angles in this experiment does not prove conclusively that the acoustic wavefront produced by the laser pulse was directional.

B. RANGE DEPENDENCE

The next experiment conducted was designed to test the expected 1/r dependence of the acoustic pressure using the high frequency hydrophone. This experiment was performed by moving the hydrophone away from the laser spot along the 30^o line where the largest pressure response was achieved. Since a high speed camera was not available to determine the distance between the laser spot and the hydrophone, the distance was calculated by dividing the nominal speed of sound in fresh water of 1480m/s by the difference between the time the acoustic pulse reaches the hydrophone and the time of the laser pulse. The time it takes the laser pulse to reach the water is negligible. Therefore, this approach underestimates the distance since the speed of the initial shock wave is higher than the speed of a linear sound wave. However, since the shock waves from laser

pulses of this magnitude are expected to dissipate at fairly short ranges, this should be a fairly good estimate several centimeters from the laser spot. For example, if the shock wave travels at 4000m/s and dissipates to a linear wave within the first centimeter of travel, the error in the distance estimate would be about 13% at 5cm. The error decreases to 6% at 10cm. The results are shown in Figure 15. The plot shows the expected roughly 1/r dependency.

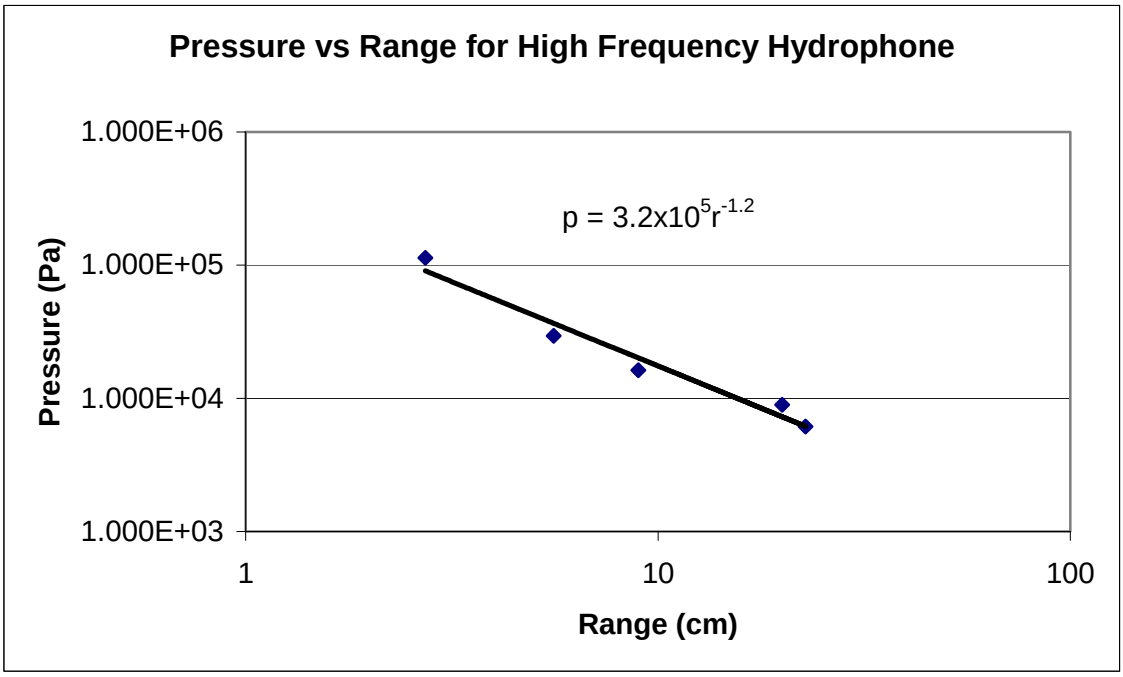

Figure 15 Determination of the 1/r dependence of the acoustic pulse using high frequency hydrophone on a log-log plot.

The variation of pressure with range was also checked using the low frequency hydrophone. The results are shown in Figure 16. A point of interest in this figure is that the pressures are two orders of magnitude lower than those from the high frequency hydrophone. This is explained by the fact that the frequency of the acoustic pulse is well above the calibrated range of the low frequency hydrophone as seen in the calibration curve in the Appendix. Despite this problem, the measured pressure still shows the same roughly 1/r range dependence.

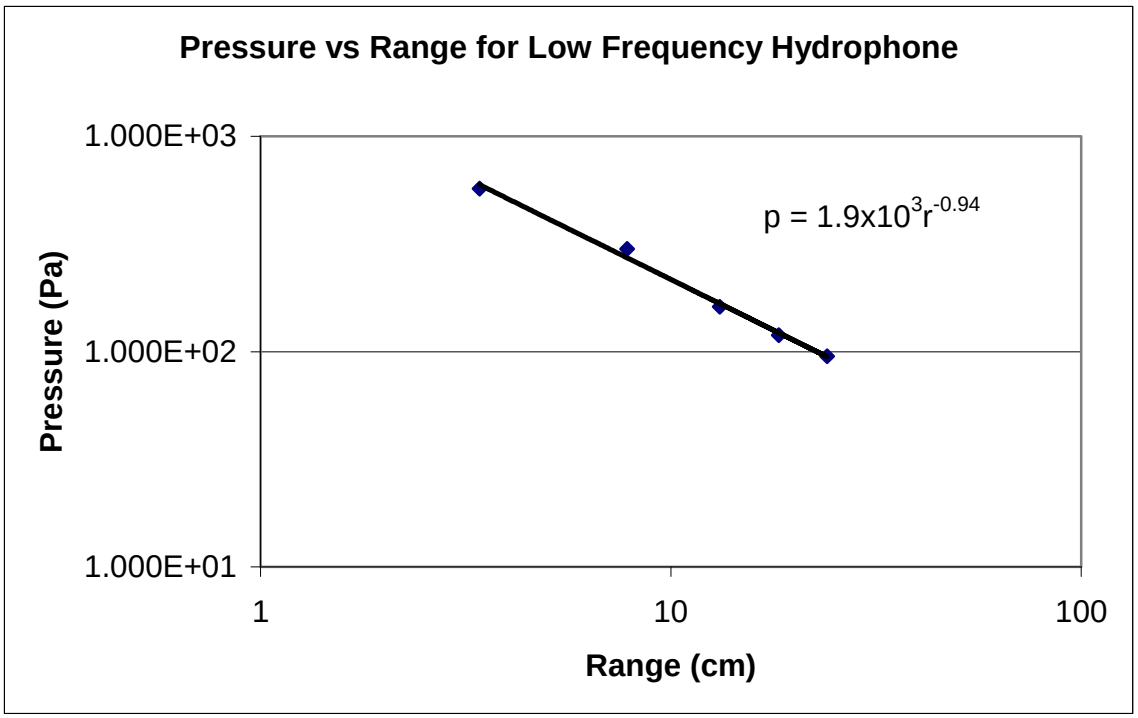

Figure 16 Determination of the 1/r dependence of the acoustic pulse using low frequency hydrophone on a log-log plot.

Since neither the spot size produced from the laser pulse nor the size of the cavitation bubble could be determined without the use of a high speed camera, no direct comparison can be made to the pressures achieved by other research groups. However, a rough comparison can be made to Vogel's results simply based on the pulse length and energy. For instance, for his experiment using a 30ps pulse length with an energy of 1mJ he got a pressure of about $1x10^5$Pa at a distance of 10cm. In the experiments conducted for this thesis, using a pulse length of about 100fs and energy of 2mJ, a pressure of about $2x10^4$Pa was obtained. This is at least consistent with Vogel's work since he found the conversion of laser energy into mechanical energy to be substantially lower for picosecond pulses as opposed to nanosecond pulses.

V. MODELS

The modeling effort in this thesis seeks to predict the characteristics of the pressure wave produced from the interaction of a high energy laser pulse in water by using an existing finite element simulation program. For this preliminary study, only the simplest of the laser parameters are used, i.e., total pulse energy, pulse length, and spot size. No attempt is made in this thesis to take into account the details of the pulse shape either temporally or spatially. It is simply assumed that the laser energy is deposited in a spherical volume uniformly over the time period of the pulse length. Likewise, interactions of the pressure wave with an air-water interface are also ignored at this point. The goal of this study is to examine the output of the finite element program in terms of peak pressure, the decrease of pressure with range, and the width of the pressure pulse. One of the biggest problems with this approach is the fact that the efficiency of the electro-optic to mechanical energy conversion is not understood well enough to be modeled. Therefore, the only alternative is to adjust the total pulse energy until the pressure matches the experimental value. The output then gives a prediction of the conversion efficiency, which can be compared with experimental values. This relatively modest goal shows the basic ability of the simulation program to handle this extremely non-linear process.

The first computer program used was a finite element program called COMSOL Multiphysics. Along with the basic multiphysics program, COMSOL also has add-on modules, which are tailored for specific applications. For example, the Acoustics Module contains built-in application modes and boundary settings for the modeling of acoustic wave propagation in solids and fluids. COMSOL also provides the ability to modify the equations of state of the materials of interest. The problem is that the deposition of high energy laser energy is highly nonlinear. COMSOL could conceivably handle the highly nonlinear physics, but it would have required heavy modification of the physics equations.

To avoid the difficulty of having to input the equations needed to handle this non-linear process, another finite element program, AUTODYN, was chosen for the modeling effort. AUTODYN software is designed for modeling the nonlinear dynamics of solids, fluids and gas as well as their interactions. Its strong point is the modeling of explosions. The efficient generation of sound by laser energy involves the formation of a plasma with an extremely high energy density. It is essentially a small explosion. Therefore, it was decided that AUTODYN would be a better choice for this application. The following sections will discuss three different approaches, which were attempted before finally settling on the final approach. Comments are provided as to the difficulty with these alternative approaches. The final approach involved simulating the laser pulse as a detonated high energy explosive. Various results of this method are discussed.

A. RADIAL VELOCITY APPROACH

The first approach was an attempt to model the results of Vogel et al. [1996] by using the radial velocity of the wall of the cavitation bubble. The 6ns, 10mJ laser spot had a diameter of 7.6μm and a shape that was approximately spherical. Vogel predicted the velocity of this wall as a function of time by using the Gilmore model of cavitation bubble dynamics and by requiring the solution to yield a maximum bubble radius conforming to the experimental value. He also measured the bubble wall velocity experimentally. The calculated maximum bubble wall velocity was 1106m/s, and the experimental value was approximately twice as high at 2450m/s. This discrepancy was attributed to the failure of the Gilmore model to model the shock front accurately. Interestingly, the calculated shock wave pressure at 1mm was higher than the experimental value. The numerical calculation yielded a pressure at the shock front of about 70MPa while the measured shock wave pressure at 1mm was 20MPa. These values agree within an order of magnitude.

To begin the modeling process, a rigid sphere of the above mentioned diameter was created in AUTODYN and surrounded by water. While creating this sphere, AUTODYN allows the user to select the equation of state that will be applied to the materials in the problem. In this case, the shock equation of state, as defined by the

Rankine-Hugoniot equations, was chosen to model the pressure wave produced in the water as a result of this expanding sphere. During this phase, the user also decides how the problem will be meshed. Meshing is the process of dividing the materials in the problem into many small pieces (finite elements) to which the program will perform calculations to determine the properties of the overall problem. For this problem, a variable mesh was used which divided the material of the rigid inner sphere corresponding to the expanding bubble and the water close to the sphere into much smaller pieces than the material further away. This was done to minimize the run time of each trial while maintaining the accuracy of the calculation close to the sphere.

AUTODYN also allows the user to choose from predefined boundary conditions. The "Flow Out" boundary condition was chosen for the outer surface of the water since this would most closely mimic an infinite boundary. AUTODYN also allows the user to input an initial condition to any material in the problem. In this case, the material in the sphere was given an initial condition of a constant, expanding radial velocity. The next step of the problem setup is to put gauges into the problem that will measure the desired parameters. The figure produced by AUTODYN for an initial radial velocity of 1107m/s is shown in Figure 17 at time 1.502 μs after the initiation of the problem. In this case, a circular outer material with a radius of 2500 μm was created surrounding the inner sphere with a radius of 3.8μm. In the figure one can see the position of the gauges (labeled 1 and 2), the pressure contours, and the units used in calculations. The shock pressures produced in this case were approximately 40 kPa measured at 250μm. Using the expected 1/r relation for pressure dissipation below 100MPa leads to about 10kPa at 1mm. These pressures are approximately three orders of magnitude lower than those measured by Vogel and his colleagues.

Trials were then conducted with radial velocities up to 5000m/s with no appreciable increase in maximum pressure. The fact that an increase in radial velocity does not result in a corresponding increase in maximum pressure with this method suggests a fundamental flaw in this approach. Therefore, the decision was made to abandon this method and try something different. It is possible that this approach could

be refined by using different equations of state or by changing the radial velocity to match the time dependence reported by Vogel. However, since Vogel et al. report that the shock wave detaches immediately following plasma formation, it is not clear that the bubble wall velocity alone can be used to predict shock wave pressures.

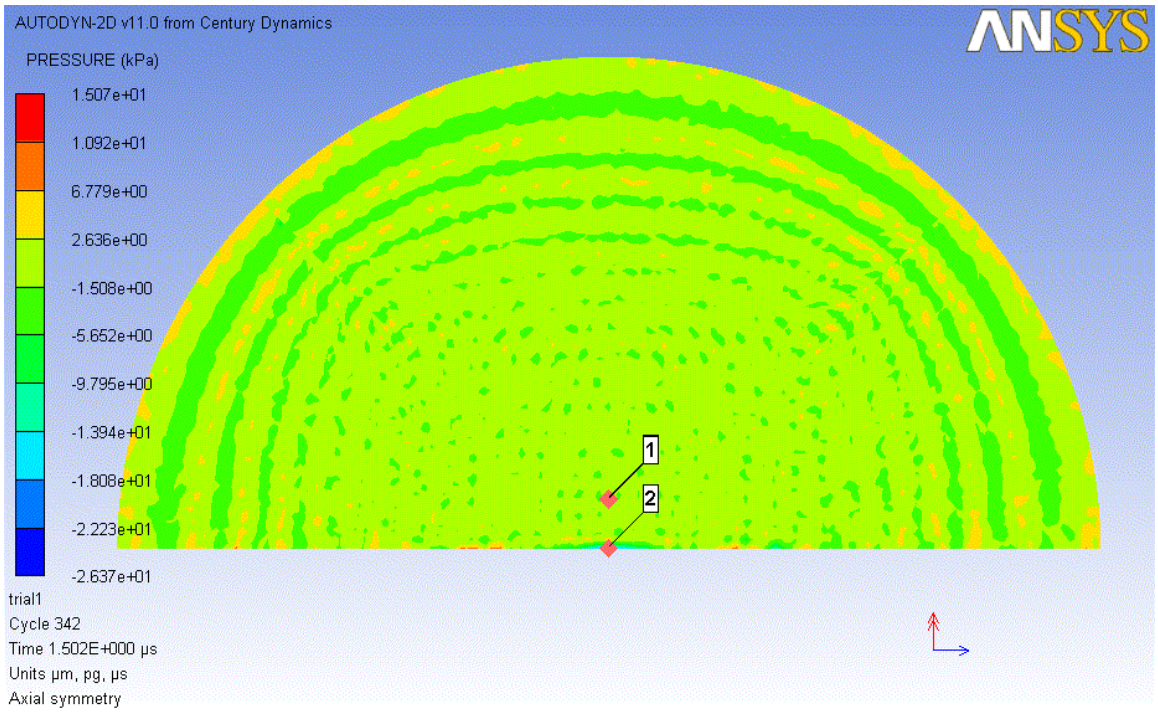

Figure 17 Example output from AUTODYN

B. INTERNAL ENERGY APPROACH

The next approach was to investigate the possibility of adjusting the internal energy of the modeled spot to match the internal energy produced by laser pulse. Since the units for internal energy in AUTODYN are J/kg, the value for internal energy was calculated by dividing the laser pulse energy by the mass of the water in the volume of the laser spot. The next step is to construct the problem as described in the previous section. The first problem encountered here was in the choice of materials. Since only a small portion of the energy added to the sphere is required to vaporize it, the sphere could reasonably be modeled as water vapor. However, AUTODYN does not have a pre-

defined choice for water vapor in its materials library. Therefore, the volume was modeled with air since, as a gas, it was judged to be the best match for water vapor. Since air was used in the inner volume, the ideal gas law equation of state was used for that volume. Again, the shock equation of state was chosen for the surrounding water since the evolution of the pressure wave from this energy density is expected to yield shock waves. The pressure pulse produced from this approach is shown below.

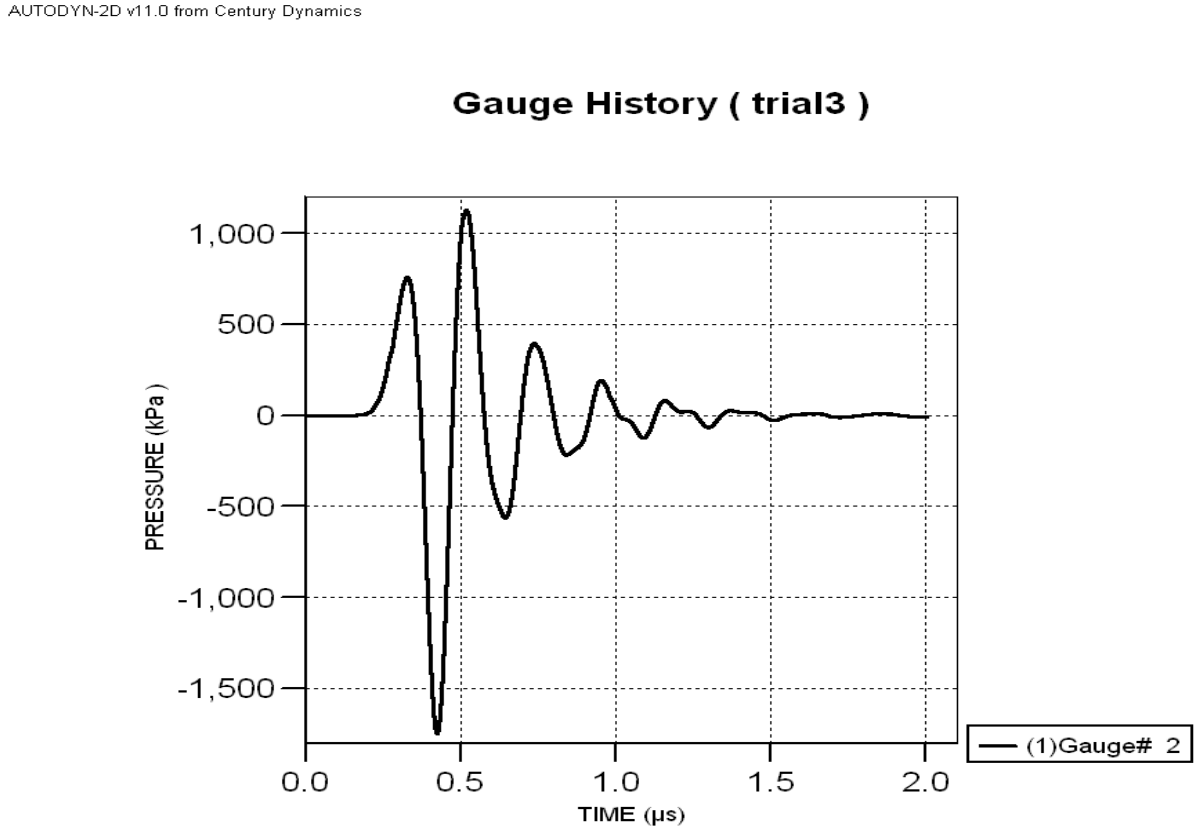

Figure 18 Pressure vs. Time for a gauge 500 µm from center of laser spot.

This pulse shape looks promising in that it has a roughly bipolar shape. Negative absolute pressure swings are realistic when quick pulses put the liquid into tension before it has a chance to react mechanically. However, the temperature profile for this run, shown in Figure 19, is unrealistic in that it predicts temperatures on the order of -10^7K. It is considered likely that this result represents a failure of the Rankine-Hugoniot equation

of state to model the full range of conditions inherent in this approach. The physically nonsensical result might follow from extrapolating the equation of state into regimes in which it is no longer valid.

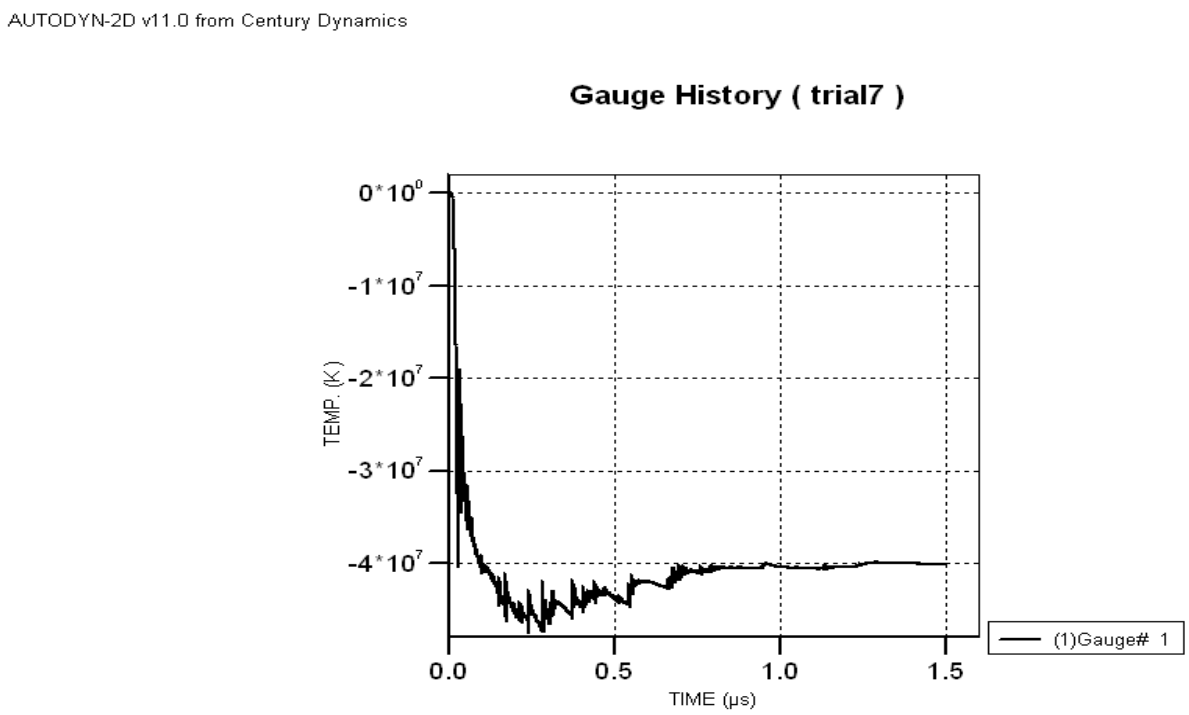

Figure 19 Temperature profile for internal energy approach.

C. OVERPRESSURE APPROACH

The next approach at the modeling effort was to try to produce an overpressure in the laser spot volume. Unfortunately, there was no direct way to do this in AUTODYN. Initial pressure is not an input option; however, density is. Thus, an attempt was made to trick AUTODYN into an overpressure situation by using the ideal gas equation of state in an air bubble with a high density. The density required was calculated as:

$$\rho = \frac{PM}{RT}, \qquad \text{Eqn 38}$$

where P is the pressure of the bubble, M is the molar mass, R is the ideal gas constant, and T is the absolute temperature. The temperature of the bubble was calculated by

assuming that all the energy of the laser pulse had been transformed into heat energy and no work had been done on the surrounding fluid. This overestimates the temperature. Figure 20 shows the result of this method for one of the trials. The difference between this plot and the one obtained with the internal energy approach is readily apparent. The pressure wave starts with a negative spike. This would be expected from an imploding bubble, but it is not expected from an overpressure situation. Curiously, however, the pressure produced is close to the order of magnitude of the pressure produced in the Vogel experiment. This prompted some further investigation into this approach.

To start, pressures between 10^5Pa and 10^6Pa were converted to density. The results of this conversion are shown in the table below. The maximum pressures produced were then plotted as a function of the increasing density. The results are shown in Figure 21. These trials did not produce the expected results. As density increases, the maximum pressure of the resulting wave decreases. These results imply that trying to create an overpressure in the laser spot by adjusting the initial density actually produces an imploding bubble. Therefore, this approach of trying to trick AUTODYN into an overpressure situation was abandoned.

Table 4 Pressure / Density used for overpressure trials

Pressure (Pa)	Density (g/cm3)
1.00E+05	7.95E-04
2.00E+05	1.59E-03
3.00E+05	2.39E-03
4.00E+05	3.18E-03
5.00E+05	3.98E-03
6.00E+05	4.77E-03
7.00E+05	5.57E-03
8.00E+05	6.36E-03
9.00E+05	7.16E-03
1.00E+06	7.95E-03

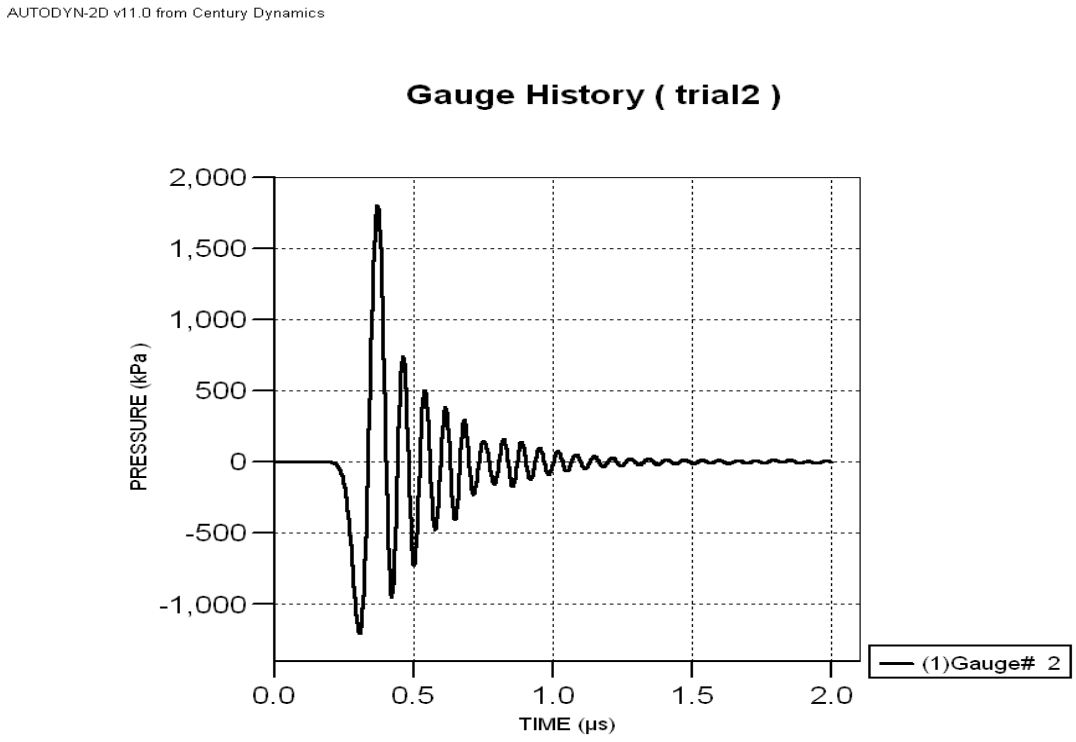

Figure 20 Pressure vs. time 500 µm from center of laser spot obtained with the overpressure approach

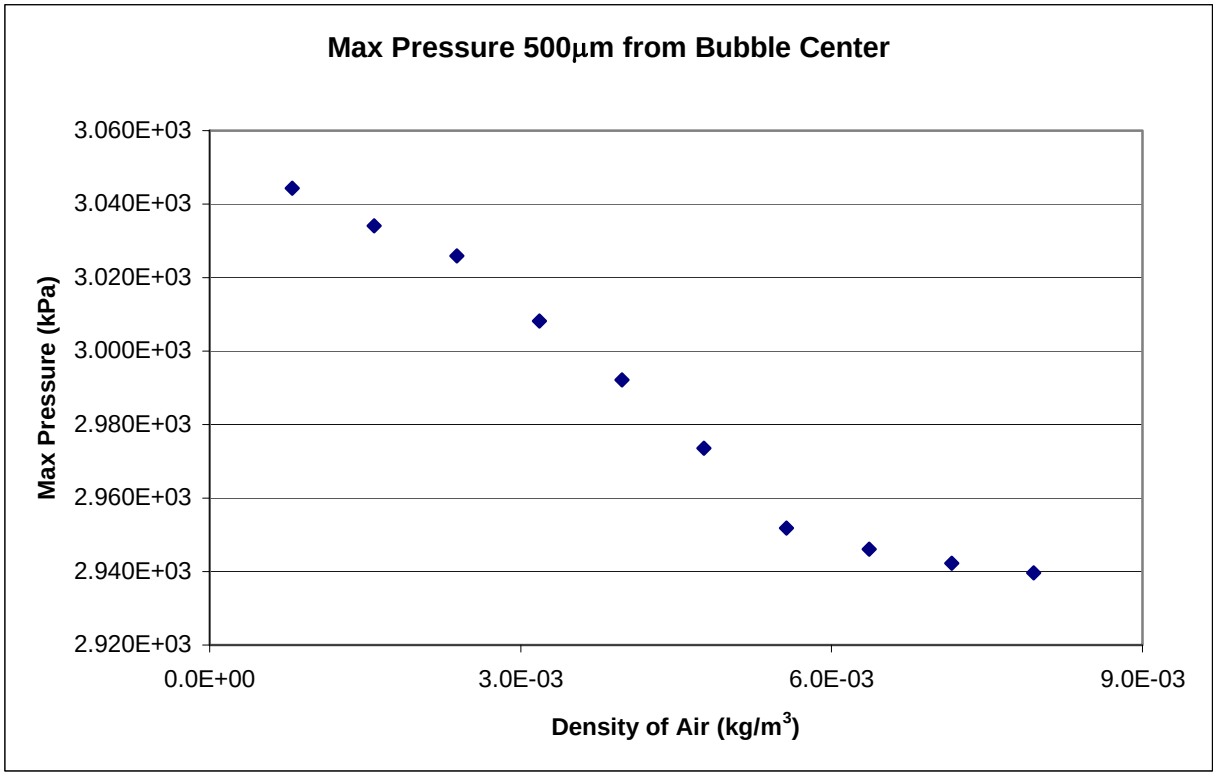

Figure 21 Maximum pressure vs. density of air 500 μm from bubble center

D. HIGH ENERGY EXPLOSIVE APPROACH

The final approach was an attempt to use a high energy explosive to create the overpressure condition desired. This method consisted of filling the laser spot volume with nitroglycerine and igniting the explosive. Again, a sphere with a radius of 3.8 μm was used in an attempt to model Vogel's 10mJ 6ns results. The resultant pressure pulse is shown in Figure 22, which was measured at 37 μm, the distance determined by Vogel to be the maximum extent of the plasma radius. Of note here is that the pressure pulse is no longer bipolar. Rather, the pressure pulse has the same shape that the higher amplitude pulses showed in Maccabee's work [1987]. At these amplitudes, a negative pressure swing cannot occur near the surface, because the water cannot withstand the tension. Instead, the pressure decreases after the initial shock wave passes with an exponential tail.

The first step of this approach was to try to get the AUTODYN generated pressure pulses to be approximately the same as those produced by Vogel. To do this, the initial internal energy of the explosive was adjusted until it produced results that matched the measure pressure at the plasma rim from Vogel's experiment. As done before, the energy in the laser spot was calculated by dividing the 10mJ laser energy by the mass in the laser spot volume with a radius of 3.8 μm to get $1x10^{11}$J/kg. Then the initial internal energy of the nitroglycerine was adjusted until the magnitude of the pressure pulse produced was approximately the same as produced by Vogel. This led to an internal energy of $8.7x10^{9}$ J/kg.

The temporal pulse length predicted by the model was also examined. To determine the pulse length from Figure 22 the point where the pulse decayed to the 1/e point was used. From this, it was determined that the pulse length was about 0.5 ns measured at 37 μm from the center. The same method was used to determine the pulse length for both the numerical calculation and experimental data from Vogel, which were about 15ns and 200ns respectively. In Vogel's work, the numerical calculation was for the pressure inside the bubble during the initial phase of bubble expansion, and the experimental data was measured 10mm from the emission center. It is expected that a pressure pulse will spread out as it travels, but measurements were not taken that far from the emission center in this model. Further work is required to examine the model parameters which contribute to the pulse length and to determine the expected pulse length at greater distances from the center.

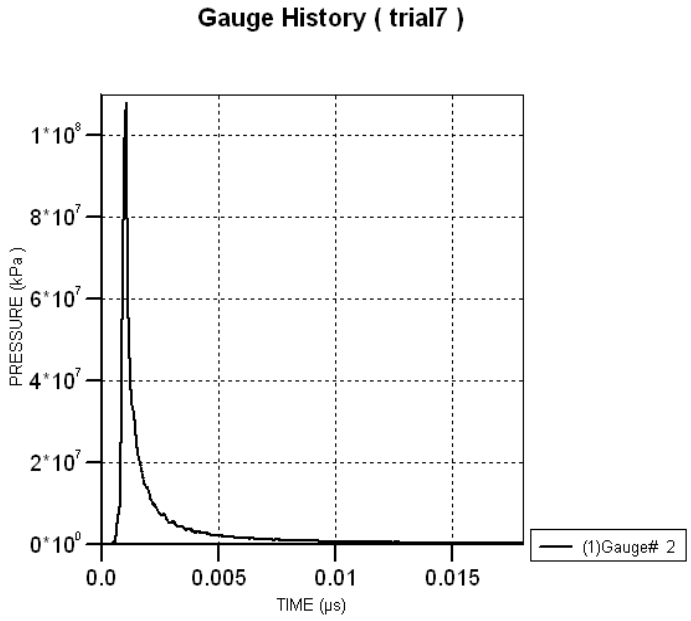

Figure 22 Pressure pulse from high energy explosive trial for the 10mJ 6ns case for a sphere with a radius of 3.8 µm measured at 37 µm from the center (edge of the plasma rim determined by Vogel).

To get the efficiency of this model, the internal energy of the nitroglycerine required to achieve the desired pressure magnitude was divided by the energy of the laser spot, which resulted in the same pressure. The result was an efficiency of 9%. This efficiency is comparable to the 6-13% efficiency from Vogel and the 10% efficiency from Jones. As one can see by comparing Figure 23 and Figure 24 the pressures from the model and from Vogel are both on the same order. Figure 23 also shows the roughly $1/r^2$ dependence that is expected of shock wave dissipation at pressures greater than 100MPa.

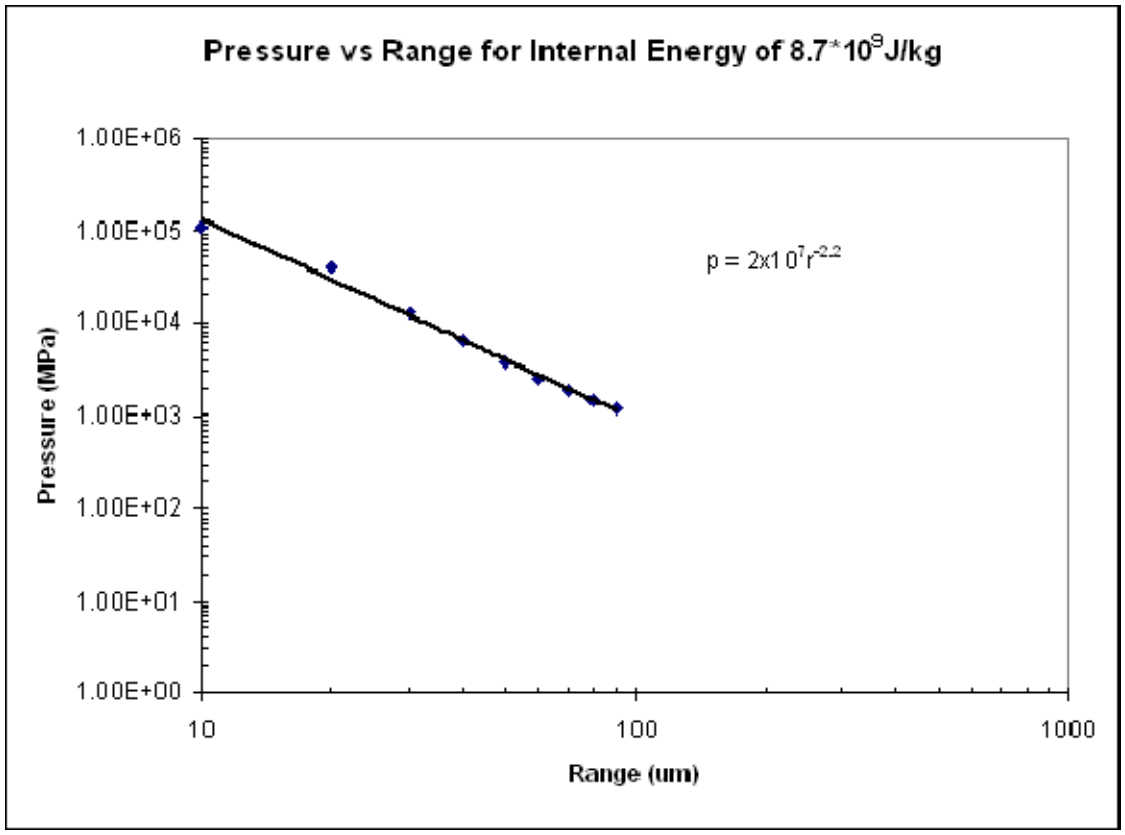

Figure 23 Pressure vs. range from AUTODYN model showing $1/r^2$ behavior from shock wave dissipation.

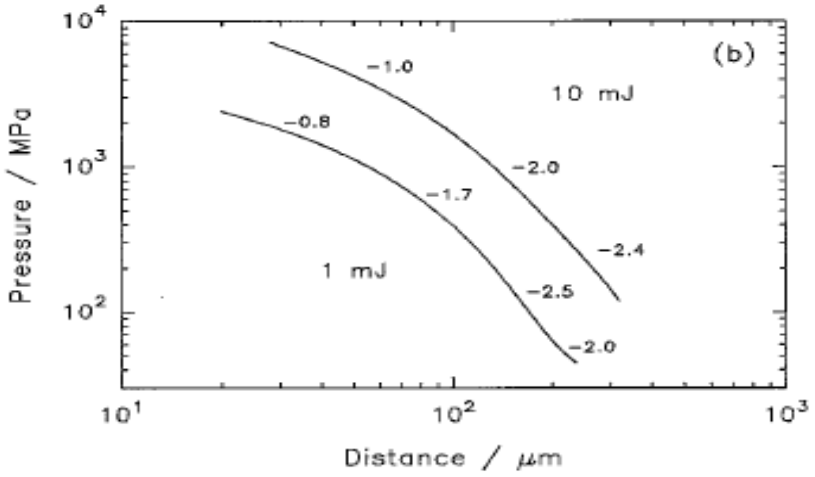

Figure 24 Pressure vs. Range from Vogel for 6ns pulse of 1mJ and 10mJ.

VI. CONCLUSIONS

In the experimental portion of this thesis, a couple of fundamental characteristics of the acoustic source were investigated. First, the directionality of the source was considered. At first glance, it seemed that the source was quite directional. Further investigation led to the conclusion that the reason for the directionality of the source was most likely due to interference between the direct acoustic pulse and its reflection off the surface.

The next result of the experimental section was the determination of the range dependence of the acoustic source. Five measurements of the peak pressure amplitude were taken at ranges varying from about 3 cm to 24 cm using both high and low frequency hydrophones. The dependence of the peak pressure amplitude with range was measured as $r^{-1.2}$ with the high frequency hydrophone and as $r^{-0.94}$ with the low frequency hydrophone. These measurements showed that the laser generated acoustic source produced the approximately 1/r range dependence expected for pressures under 100MPa.

The modeling aspect of this thesis also produced some interesting conclusions. To start, it was determined that AUTODYN handled the nonlinear aspects of this thesis better and was easier to use than COMSOL. It also showed that, although there were many possible approaches within AUTODYN to model the acoustic source, it was determined that the best results came from modeling the laser generated acoustic source as a sphere of nitroglycerine with adjusted internal energy. This method led to a couple of positive results. The first was the calculated efficiency was comparable to that of the main references used in this thesis. Comparing the adjusted internal energy to the calculated internal energy of the laser spot led to an efficiency of 8.7%. This efficiency is comparable to the 6-13% efficiency from Vogel and the 10% efficiency from Jones. The model also showed the range dependence of the peak pressure amplitude of the pulse to be $r^{-2.2}$ from 10 to 100 μm. This is in agreement with the roughly $1/r^2$ relationship of pressure vs. range that is expected in the strong shock wave regime. This method also

produced a pulse length of about 0.5ns measured at 37 μm, which is the maximum extent of the plasma as determined by Vogel. This value for pulse length is within about an order of magnitude of the 15ns pulse length calculated inside the plasma produced by the numerical analysis done by Vogel.

VII. RECOMMENDATIONS FOR FOLLOW-ON WORK

Although this thesis shows the promise of a laser generated acoustic source there is still a lot of work that needs to be done. One of the questions that arose from the theory section had to do with the plasma frequency. If the energy density is too high, electron densities may be high enough to exceed the plasma frequency. In this case, all remaining electro-optic energy would be reflected. Thus, the upper limit to the energy density is determined by the point where the plasma frequency is reached. Further investigation needs to be done to determine the highest energy density before plasma frequency is reached, and how does the pulse shape affect the point where the plasma frequency is reached?

Another point for further investigation will be the interaction between multiple pulses. Due to the need for an acoustic signal in the hundreds of kilohertz, work will need to be done to determine how each successive laser pulse will interact with the bubbles and heating produced by previous laser pulses. This effort will need to include a study of the refraction of sound in the water heated from successive laser pulses and also the potential scattering of acoustic waves off of the bubbles formed.

The next area for follow-on work comes from the modeling aspect. Work needs to be done to determine if modeling the laser generated acoustic source as a sphere filled with an explosive is the most realistic means of modeling this problem. The model also needs to be expanded so that the pressure pulse can be measured much further from the laser spot to determine if the pulse length result produced by Vogel at 10mm can be reproduced. Once that is determined, the next step will be to determine a way to model multiple pulses and to see if AUTODYN can predict the way multiple pulses will interact with each other.

Finally, the question of efficiency must be addressed. For example, the efficiency of the free electron laser is expected to reach about 10%. Combined with a conversion efficiency for the electro-optic to acoustic process of approximately 10%, this leads to an overall efficiency of 1%. Further studies of the potential advantages of a laser source are required to determine whether they outweigh the disadvantage of this low efficiency and to compare the cost with more traditional acoustic sources.

APPENDIX.

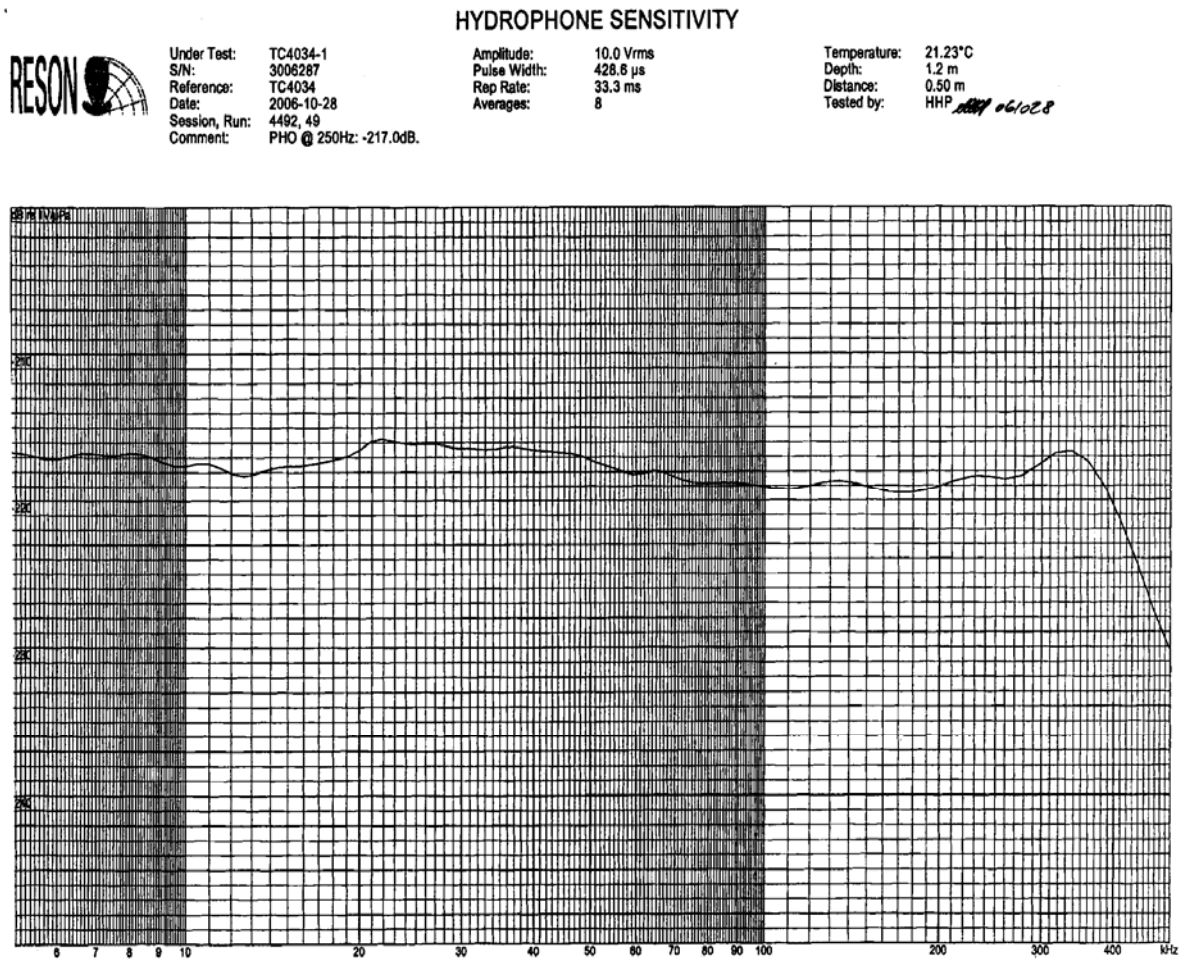

Figure 25 Low Frequency Hydrophone Sensitivity. Sensitivity in dB re 1V/µPa vs. frequency on a linear-log plot.

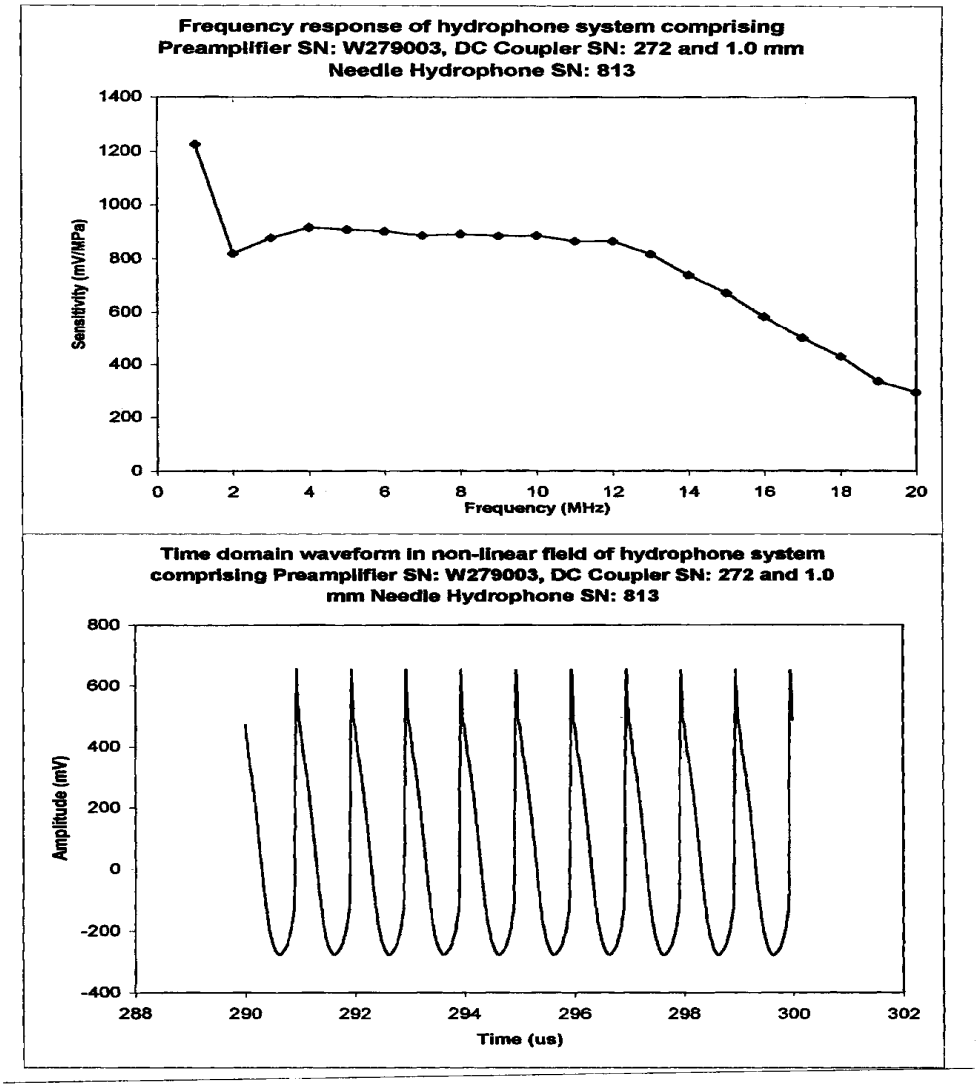

Figure 26 Sensitivity of Needle Hydrophone with serial number 813.

Table 5 Calibration data showing sensitivity and uncertainty at each frequency for hydrophone with serial number 813.

FREQUENCY RESPONSE CALIBRATION DATA

Device Identification		**In-House Preamplifier and DC Coupler**	
Preamplifier SN	W279003	**Hydrophone Diameter**	1.0 mm
DC Coupler SN	272	**Hydrophone Type**	Needle
		Hydrophone SN	813

Frequency (MHz)	Sensitivity (mV/MPa)	Uncertainty(%)
1	1225.6	14
2	819.1	14
3	878.8	14
4	916.2	14
5	908.8	14
6	903	14
7	887	14
8	892.3	14
9	886	15
10	887.2	15
11	865.2	16
12	865.6	17
13	817.3	18
14	739.2	19
15	672.2	20
16	582.3	22
17	498.3	25
18	428.9	32
19	335.3	34
20	293	38

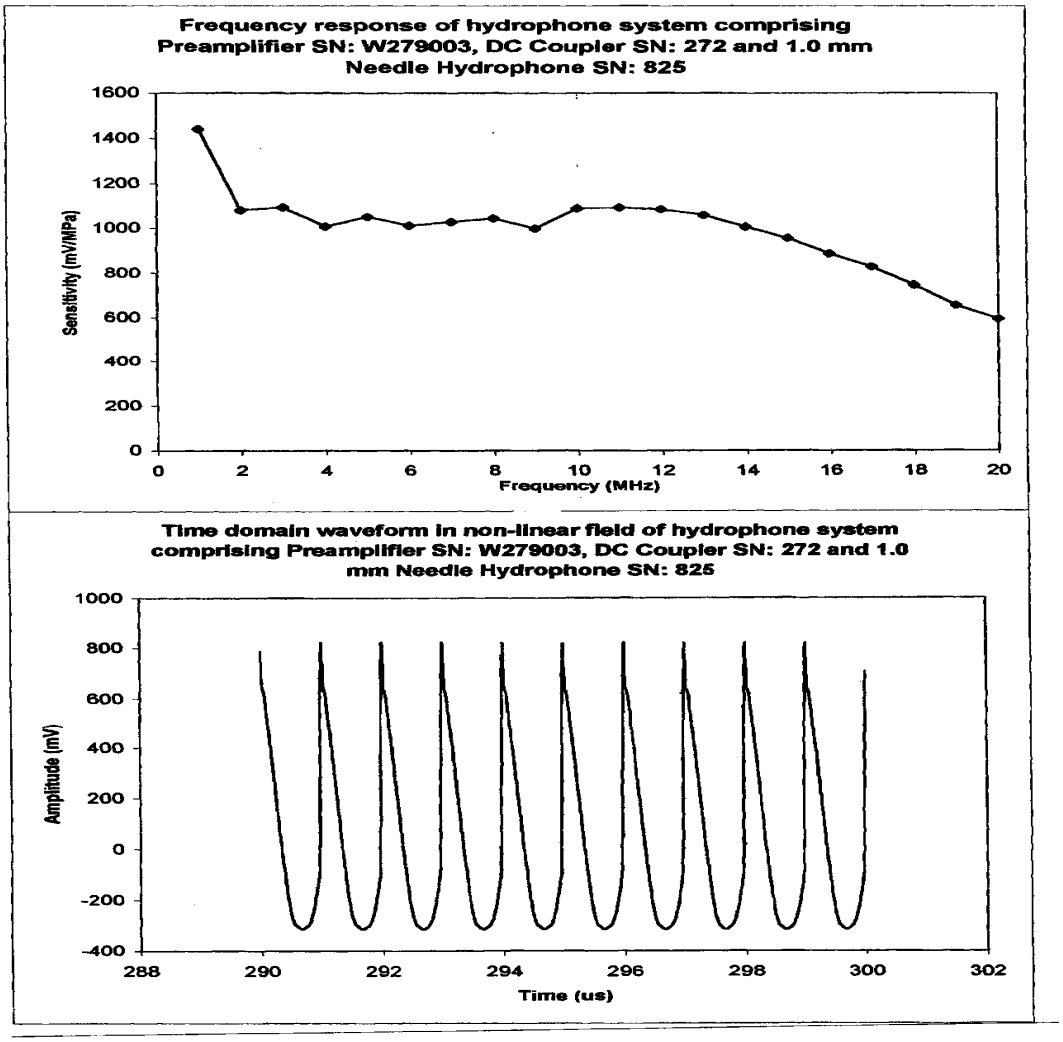

Figure 27 Sensitivity of Needle Hydrophone with serial number 825

Table 6 Calibration data showing sensitivity and uncertainty at each frequency for hydrophone with serial number 825.

FREQUENCY RESPONSE CALIBRATION DATA

Device Identification		**In-House Preamplifier and DC Coupler**	
Preamplifier SN	W279003	**Hydrophone Diameter**	1.0 mm
DC Coupler SN	272	**Hydrophone Type**	Needle
		Hydrophone SN	825

Frequency (MHz)	Sensitivity (mV/MPa)	Uncertainty(%)
1	1441.6	14
2	1081	14
3	1094.1	14
4	1006.8	14
5	1050.2	14
6	1011.7	14
7	1027.6	14
8	1042.8	14
9	998.5	15
10	1088.1	14
11	1092.7	15
12	1083.5	15
13	1057.9	15
14	1005.9	15
15	954.6	15
16	887	16
17	827.2	18
18	747.7	18
19	654.2	19
20	592	19

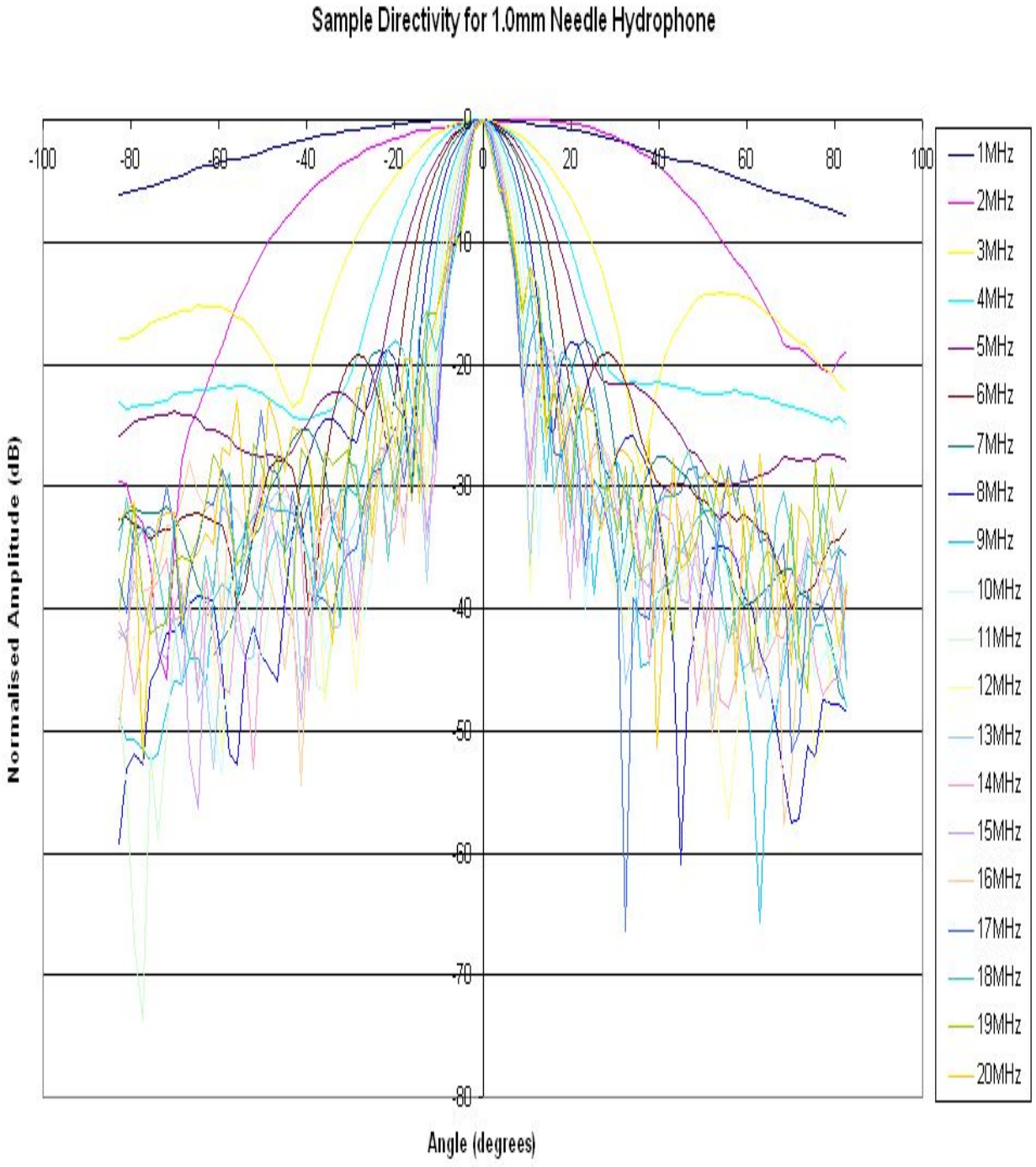

Figure 28 Directivity for needle hydrophones

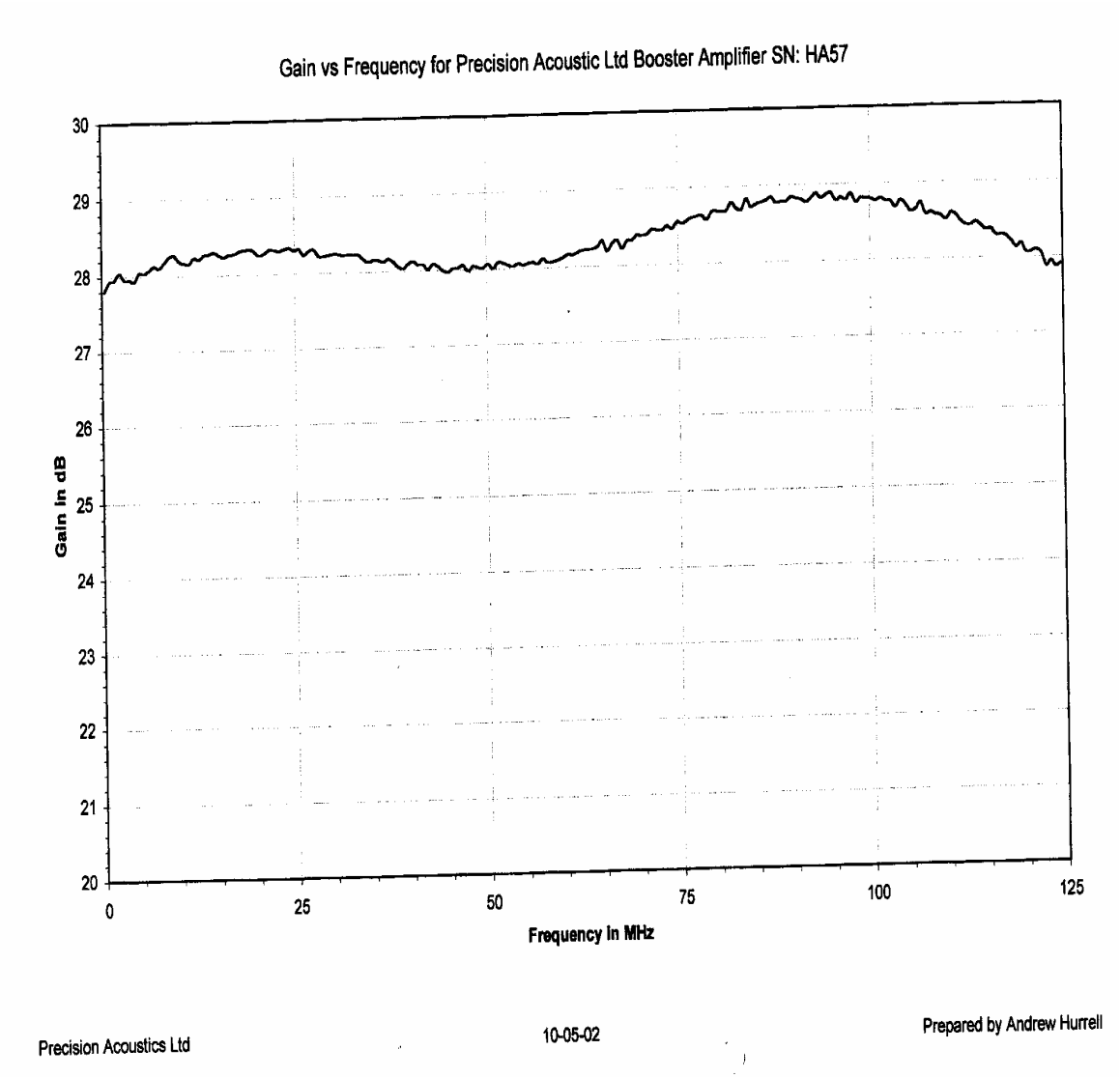

Figure 29 Gain vs. frequency for booster amplifier HA57

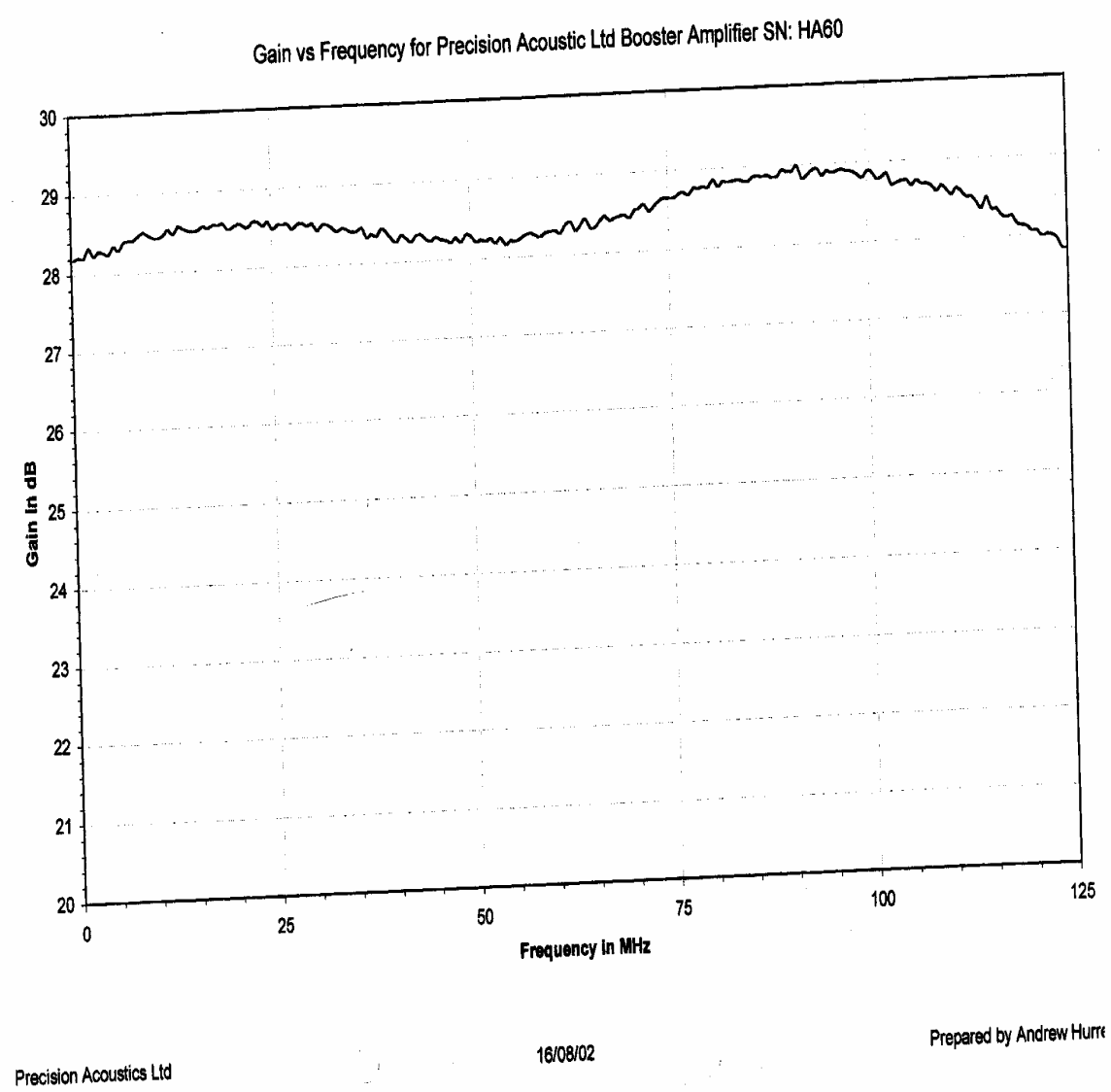

Figure 30 Gain vs. frequency for booster amplifier HA60

LIST OF REFERENCES

AUTODYN. 08 January 2008. http://www.ansys.com/products/autodyn.asp.

Berthelot, Y. H. and Busch-Vishniac, I. J. (1985). Laser-induced thermoacoustic radiation. *Journal of the Acoustic Society of America,* volume 78(issue 6). pp. 2074 – 2082.

Berthelot, Y. H. and Busch-Vishniac, I. J. Optical generation of sound: Experiments with a moving thermoacoustic source. The problem of oblique incidence of the laser beam. ICA Associated Symposium on Underwater Acoustics; Halifax; N.S. (Canada); 16-18 July 1986. pp. 603 - 610. 1986.

COMSOL. 08 January 2008. http://www.comsol.com/products/multiphysics/.

Federation of American Scientists. AN/SLQ-25 NIXIE. 08 January 2008 http://www.fas.org/man/dod-101/sys/ship/weaps/an-slq-25.htm.

Gorodetskii, V.S., Egerev, S. V., Esipov, I. B. and Naugol'nykh, K. A. (1978) Generation of sound by laser pulses. Sov. J. Quantum Electron., 8(11) November 1978. pp. 1345 – 1347.

He, H. and Feng, S. (1999). Ultrashort Pulse Laser Used to Generate Sound Under Water. Shanghai Acoustics Laboratory, Chinese Academy of Science.

Jones, T. G., Grun, J., Bibee, D., Manka, C., Landsberg, A. and Tam, D. (2003) Laser-generated shocks and bubbles as laboratory-scale models of underwater explosions. *Shock and Vibration*, volume 10 (2003). pp. 147 – 157.

Jones, T. G., Grun, J. and Manka, C., (1999) Feasibility Experiments for Underwater Shock and Bubble Generation with a High-Power Laser, Naval Research Laboratory Technical Report, NRL/MR/6790-99-8317, 22 April 1999.

Jones, T. G., Ting, A., Penano, J., Sprangle, P. and DiComo, G. (2006) Remote Underwater Ultrashort Pulse Laser Acoustic Source. Combined Conference on Lasers and Electro-Optics, Quantum Electronics and Laser Science Conference, Conference on Photonic Applications, Systems, and Technologies. May 21-26, 2006.

Jones, T. G., Ting, A., Penano, J., Sprangle, P., Nicholas, M., McDonald, E., Bibee, D. and Lindwall, D. (2007). Remote Intense Laser Acoustic Source. Briefing to NAVSEA, 10 January 2007.

Maccabee, B. S. (1987). Laser Induced Underwater Sound. *1987 Ultrasonics Symposium.* pp. 1099 – 1108.

Pierce, A. D. and Hsieh, H. A. Underwater Soundbeams Created by Airborne Laser Systems. ICA Associated Symposium on Underwater Acoustics; Halifax; N.S. (Canada); 16-18 July 1986. pp. 595 - 602. 1986.

Sulak, L., Armstrong, T., Baranger, H., Bregman, M., Levi, M., Mael, D., Strait, J., Bowen, T., Pifer, A.E., Polakos, P. A., Bradner, H., Parvulescu, A., Jones, W. V. and Learned, J. (1979) Experimental Studies of the Acoustic Signature of Proton Beams Traversing Fluid Media. Nuclear Instruments and Methods 161 (1979). pp. 203-217.

Vogel, A., Busch, S. and Parlitz U. (1996). Shock wave emission and cavitation bubble generation by picosecond and nanosecond optical breakdown in water. *Journal of the Acoustic Society of America,* volume 100 (issue 1). pp. 148 – 165.

Vogel. A., Noack, J., Nahen, K., Theisen, D., Busch, S., Parlitz, U., Hammer, D. X., Noojin, G. D., Rockwell, B. A. and Birngruber, R. (1999). Energy balance of optical breakdown in water at nanosecond to femtosecond time scales. *Applied Physics B. Lasers and Optics,* volume 68. pp. 271 – 280.

INITIAL DISTRIBUTION LIST

1. Defense Technical Information Center
   Ft. Belvoir, Virginia

2. Dudley Knox Library
   Naval Postgraduate School
   Monterey, California

3. Professor Daphne Kapolka
   Department of Physics
   Naval Postgraduate School
   Monterey, California

4. Ted Jones
   Naval Research Laboratory, Code 6795
   Washington D.C.

5. Professor Kevin B. Smith
   Department of Physics
   Naval Postgraduate School
   Monterey, California

6. Capt. Dave Kiel
   Pers 405, NAVSEA
   Washington D.C.